Journal of Archaeological Science: Reports, Volume 49, June 2023, Article number 103980
DOI: 10.1016/j.jasrep.2023.103980

Middle Neolithic fluorites in Northern France and Belgium: characterization, sourcing and methodological limitations

Eric Goemaere[a,*], Bart Vanmontfort[b], Dominique Bonjean[c], Dominique Bosquet[d], Françoise Bostyn[e], Nicolas Cayol[f], Caroline Colas[g], Hélène Collet[h], Thomas Delbey[i], Emmanuel Delye[j], Mark Golitko[k], Ivan Jadin[l], Cécile Jungels[m], Emmanuelle Leroy-Langelin[n], Cécile Monchablon[o], Ivan Praud[p]

[a] Geological Survey of Belgium, OD Earth and History of Life, Royal Belgian Institute of Natural Sciences, 26, rue Vautier, 1000 Brussels, Belgium
[b] KU Leuven, Dept. Archaeology, Centre for the Archaeological Research of Landscapes, Celestijnenlaan 200E pb 2409, 3001 Heverlee (Leuven), Belgium bart.vanmontfort@kuleuven.be
[c] Centre archéologique de la grotte Scladina, ASBL Espace muséal d'Andenne, 339D, rue Fond des Vaux, 5300 Sclayn, Belgium Dominique.Bonjean@ema.museum
[d] Agence Wallonne du Patrimoine – Direction de la coordination opérationnelle, 44, rue du Moulin de Meuse, 5000 Beez (Namur), Belgium dominique.bosquet@awap.be
[e] Université de Paris 1, UMR 8215, 9, rue Malher, 75004 Paris, France Francoise.Bostyn@univ-paris1.fr
[f] INRAP, Avenue du Parc, Parc d'activités Noyon-Passel, 60400 Passel, France. UMR 8215 « Trajectoires-De la sédentarité à l'Etat », Paris, France nicolas.cayol@inrap.fr
[g] INRAP Nord Picardie UMR8215 Trajectoires, Impasse du Commandant Gérard, 02200 Soissons, France caroline.colas@inrap.fr
[h] Agence Wallonne du Patrimoine, Direction opérationnelle de la Zone Ouest, Service public de Wallonie, Station de recherche de Spiennes, 52, rue d'Harmignies, 7032 Spiennes, Belgium helene.collet@awap.be
[i] Cranfield Forensic Institute, Cranfield University, Defence Academy of the United Kingdom, Shrivenham, SN6 8LA, UK Thomas.Delbey@cranfield.ac.uk
[j] Cercle archéologique Hesbaye-Condroz, Belgium emmanuel.delye@skynet.be
[k] Department of Anthropology, University of Notre Dame, Notre Dame, The Field Museum of Natural History, Negaunee Integrative Research Center, Social Science, Chicago, USA mgolitko@nd.edu
[l] Anthropology and Prehistory, Quaternary environments and Humans, OD Earth and History of Life, Royal Belgian Institute of Natural Sciences, 29, rue Vautier, 1000 Brussels, Belgium ijadin@naturalsciences.be
[m] Préhistomuseum, Centre de Conservation, d'Étude et de Documentation, 128, rue de la Grotte, B-4400 Flémalle, Belgium Cjungels@prehisto.museum
[n] Département du Pas-de-Calais, 9 rue Whisthable, 62000 Dainville and Université de Lille, CNRS, ministère de la Culture, UMR 8164 - HALMA – Histoire, Archéologie et Littérature des Mondes Anciens, 59000 Lille, France leroy.langelin.emmanuelle@pasdecalais.fr
[o] Centre archéologique Inrap, 32 rue Delizy, 93694 Pantin cedex, France ; UMR 8215 « Trajectoires. De la sédentarité à l'État » cecile.monchablon@inrap.fr

[p] Centre archéologique Inrap, ZI de la Pilaterie, 11, rue des Champs, 59650 Villeneuve d'Ascq. UMR 8215 « Trajectoires-De la sédentarité à l'Etat », Centre de recherches, 9, rue Malher F-75004 Paris, France ivan.praud@inrap.fr

*Corresponding author. E-mail address : egoemaere@naturalsciences.be

Abstract

Ornaments and fragments of fluorite have been found at sixteen Neolithic sites in Belgium and Northern France, mainly Middle Neolithic sites associated with the Michelsberg culture and the Spiere and Chassean groups. These sites are located in a large geographical area representing different types of sites and various geological backgrounds. One of the aims of this study is to identify where this mineral could have been quarried in the Neolithic and compare the possible source(s) with those used during the Palaeolithic. A survey of some Neolithic fluorite occurrences in Belgium and Northern France was conducted and the origins of this mineral investigated by means of geochemical Rare Earth Elements and Sr-isotopic analysis. We also explore the limitations of isotopic $^{87}Sr/^{86}Sr$ and REE ratios for analysis of fluorite. Results show that Neolithic fluorite originates from different local and regional sources, mainly the Dinantian limestones/dolostones of the Ardennes Allochthon, in contrast to the use of silicified Givetian limestones of the Calestian Band near Givet (France) during the Magdalenian. The Neolithic fluorite that is studied in this paper is found exclusively at settlement sites whereas elsewhere, fluorite comes exclusively from funerary contexts.

Keywords: Fluorite ornaments, Middle Neolithic, REE, Sr isotopes, Northern France, Belgium

1. Introduction and aims

In Europe, prehistoric personal ornaments (beads, pendants, charms…) found in the archaeological record were made out of a large variety of raw materials of different composition: (1) organics of vegetal origin such as amber, wood, lignite and jet (e.g. van Gijn, 2006; Odriozola et al., 2019); (2) organics of faunal origin, for instance bone, ivory, shell, tooth, and mineralised organisms (e.g. van Gijn, 2006; Hauzeur & Cauwe, 2012); (3) rocks, for example amphibolite, "callaïs", dolerite, fibrolite, iron ores, jadeitite, limestone, micaschist, slate or steatite, and minerals like cornaline, fluorite, gypsum, quartz, malachite, pyrite sillimanite and variscite (e.g. Gaydarska and Chapman, 2008; Polloni, 2008 p.78; Hauzeur & Cauwe, 2012 p.40; Odriozola et al., 2016). Variation in raw materials also corresponds to a wide variation of colours. Minerals offer the largest palette of colours with a wide variety of shades. Transparency, translucency, reflectance, and shine are other apparent properties of some minerals. It can be assumed that these characteristics and their aesthetic value were an important factor for the selection of raw materials for ornament production in the past (e.g. Gaydarska and Chapman, 2008; Garrido-Cordero et al., 2020a, 2020b, 2021). Quartz and garnets are well-known semi-precious gemstones offering a diversity of colours (Garrido-Cordero, 2021). Fluorite, however, offers even more colours and shades (Goemaere

and Philippo, 2010). Different colours of fluorite can even be associated in a same vein, which is not the case for garnets and most other minerals.
In Europe, fluorite has been used for personal ornamentation since the Upper Palaeolithic (Garrido-Cordero et al., 2020a, 2020b), especially during the Magdalenian in Belgium (Jungels and Goemaere, 2007; Goemaere et al., 2013; Honings et al., 2014) but also in France (Enval, Vic-le-Comte, Puy-de-Dôme department; Merlet et al., 2016; Surmely, 2019). In Belgium, this mineral was worked at Chaleux cave, where 440 g of cleaved fragments were recovered, and probably distributed to the caves of Spy, "Trou Magrite" and "Trou du Frontal" (Jungels and Goemaere, 2007; Goemaere et al., 2013). Goemaere et al. (2013) determined the geological origin of Belgian Upper Palaeolithic fluorites by means of the study of Rare Earth Elements (REEs) by LA-ICP-MS chemical analysis and Sr isotopic analysis. Personal ornaments carved out of fluorite as well as raw fluorite and cleavage fragments have also been encountered in a limited number of Belgian and Northern French Neolithic sites. To our knowledge, there are no occurrences of fluorite in Neolithic contexts in Germany, The Netherlands, Luxembourg, or southern Belgium.

Infrequent Neolithic fluorites have been discovered in France outside of our study area but have never been submitted to archaeometric study of characterization and provenance. A white-green fluorite bead roughout (2x1.1x0.9 cm) was collected from the fill of a pit at "Artière-Ronzière" (Beaumont, Puy-de-Dôme, Auvergne-Rhône-Alpes region, France), dating to the Middle Neolithic II (Chassean) (Saintot, 2016). A broken fluorite bead (of unspecified colour) from a necklace was found in a Final Neolithic ossuary (culturally related to the Seine-Oise-Marne populations of the Paris Basin and to the people of the Vienne-Charente group of central-western France) discovered in the early 1960s at Éteauville (commune of Lutz-en-Dunois, Eure-et-Loir Department, Centre-Val de Loire region, France). This bead (diameter of 14.5 mm and a thickness of 6.5 mm) presents an eccentric biconical perforation (Bailloud et al., 1965). Some 35,000 ornaments made of about forty minerals or rocks, mainly talc, limestone, and calcite, were registered in more than 200 studied sites ranging from the Early Neolithic to the Bronze Age in southern France, among which less than 100 objects are fluorite beads and pendants. Only three of these sites date from the Middle Neolithic. Translucent, colourless to pale green or blueish fluorite has been identified at eleven sites, all located between Perpignan and Avignon (Provence-Alpes-Côte d'Azur region), west of the Rhône River; the Narbonne area is the most represented. Ten sites are attributed to the Final Neolithic and one to the Early Bronze Age. The source of fluorite is considered regional (Roscian et al., 1992).

In the context of the Final Neolithic to the Chalcolithic and the Bell Beaker/Early Bronze Age, small ovoid beads of green fluorite were excavated from the Mont Bouquet cave in Bouquet (Gard Department), the "Trois Chênes" caves in Rouet, Mas Colombier cave in Lunas (Hérault Department), and the dolmen of Séveyrac-l'Église (Aveyron Department). White fluorite beads are known from the cave of Haute Fournarié at Saint Hippolyte (Gard Department), the dolmen of Bosc at Saint-Antonin (Aveyron Department) as well as yellow fluorite from dolmen 2 of Feuilles at Rouet (Hérault Department), dolmen 5 of Font du Griffe at Montpeyroux (Hérault Department), and the Eastern cave of Trou des Viviès at Narbonne (Aude Department) (Barge, 1982). In a Chalcolithic and Bell Beaker context, the same author cites biconical beads of white fluorite (dolmen 2 of Pérignac in Salles-la-Source, Aveyron; dolmen of the Camp in Rouet, Hérault; dolmen 6 of the lakes in Minerve, Hérault), green fluorite (dolmen 3 of the bastide in Florac, Lozère), bluish fluorite (cave E of the Trou de Viviès in Narbonne, Aude), and pink fluorite (dolmen 1 of the Font du Griffe in Montpeyroux, Hérault), as well as some uncertain biconical specimens found in the Pont du Hasard cave in Corconne (Gard), the Trou du Loup cave in Armissan, and the Bois de Moure dolmen in Pennautier (Aude).

Five fluorite beads of different formats and sizes were found in four natural caves (Cascais, Obidos, Oeiras, Sesimbra) used as necropoli during the Late Neolithic and the Chalcolithic in Estramadura Province (Portugal) (Cardoso et al., 2012). On the Iberian Peninsula, evidence of adornments made on fluorite in Late Neolithic/Copper Age (late 4th to 2nd millennia BC) contexts are scarce and synthetised by Garrido-Cordero (2020a). Garrido-Cordero et al., (2020b) have published a global examination of spatial variability and chronological and contextual patterning of fluorite used for prehistoric ornaments during late prehistory (6th to 2nd millennia BC) in Iberia. This study includes a characterization analysis by means of p-XRF, X-ray diffraction, VIS/NIR spectrometry and p-Raman spectroscopy. Garrido-Cordero et al. (2021, p. 11) indicate, but only for peculiar archaeological finds, that “the proximity of outcrops of fluorite at (…) may support a local provenance for that mineral”.

During the Bronze Age, occurrences of archaeological fluorite are very rare in Belgium. Beex & Roosens 1963 report that the tumulus of Mol “Bergeykse Heide” contains funerary furniture in a wooden box with a bronze object and two beads, one in amber and one in segmented fluorite but the source of the fluorite was not addressed.

This leads to the question of the origin of the raw material, as fluorite outcrops were not always identified in the immediate surroundings of these archaeological sites. What time and effort were invested in the procurement of the material? Was this a precious material, exchanged over a significant distance or available in close proximity to its use? Are the sources used similar or different compared to fluorites unearthed in Upper Palaeolithic contexts? The purposes of this study are, therefore, to survey all Neolithic fluorite occurrences in Belgium and Northern France and investigate the origins of this mineral by means of geochemical and isotopic analysis.

2. Fluorite in the geological record

Mineralogically, fluorite is a fluoride of calcium (CaF_2) and belongs to the isometric system with a cubic face-centred lattice. In nature, it most commonly forms granular to massive aggregates or crystals (cubes, octahedrons, and other more complex crystalline forms). Natural fluorites exhibit rainbow colours in various shades: from colourless to white, yellow to orange, pink to purple-red, purple to violet, blue, pale green, brown or violet-black; it can be homogenous, multicoloured and banded. Purple and green are the most commonly found coloured crystals in Belgium and France. The origin of fluorite colour remains unclear and is probably influenced by several factors including crystal defects, REEs and trace elements, and in any case is related to the physico-chemical environment of formation. Its fracture is subconchoidal, but the mineral has a (very) easy and perfect cleavage on {111}, parallel to the octahedral faces and can be peeled off to smooth out a crystal into a perfect octahedron. Fluorite is soft (4 on the Moh's scale) and creates beautiful gemstone ornaments if a large enough chunk is found; faceted crystals are very popular among collectors.

Fluorite occurs worldwide in a variety of geological environments and may occur as the main ore mineral (veins, stratabound, pipe like bodies and stockworks) in deposits, or may be present as an accessory mineral in many rock types. The (geo)chemical origin of individual fluorite deposits is based on the composition of fluid inclusions and distinct geochemistry (Smith and Hurst, 1974; Magotra et al., 2017). The REE distribution patterns in ore forming fluids are of great significance for deciphering the formation conditions of fluorite deposits. Epigenic fluorite deposits in Belgium are associated with sedimentary rocks (almost entirely carbonates) and are believed to be formed by diagenetic fluids. These deposits are characterised by very low temperature of formation (100˚C - 150˚C) and mostly occur as open space fillings, collapse, and solution breccias and/or replacement within carbonate and sedimentary host rocks.

3. Materials and methods

3.1 The archaeological material

The fluorites examined in this study originate from sixteen different Neolithic settlement sites, eight in Belgium and eight in Northern France (Fig. 1). None of these artefacts are associated with burials. All sites can be dated to the late 5th and early 4th Millennium cal BC[1] and are associated with the Spiere Group, the Michelsberg culture and the northern Chassean[2] (Table 1). Fluorite occurs at these sites as shapeless fragments, (imperfect) octahedrons and cleaved fragments as well as polished and perforated beads and pendants (Figs. 2 and 3). No crystals have been observed. The colour of most objects and fragments is violet, but purplish, green, pink and colourless fluorites are also present (Figs. 2 and 3, Table 2). The number of artefacts is small: 26 worked pieces and many more fragments, with a total weight around 270 g. Most of these were found at Thieusies, with a total of hundreds of objects of different colours weighing 159 g. Only at this latter Michelsberg site do the objects represent different steps of the production chain, including small fragments, cleaved fragments, beads broken during the drilling process, and entire beads. It is the only site for which the objects can be interpreted as part of a workshop. For our archaeometric analysis, this is also the only assemblage from which several fragments could be sampled. Beads and fragments are very rare overall. Morphologically, the shape of the beads is very simple, without any specific decoration, and quite similar at all sites. The hole is always biconical, produced by rotational drilling, possibly with the use of a flint borer; such tools are present in the assemblage at Thieusies (Vermeersch et al., 1990).

---

[1] The subdivision of the Neolithic differs in different countries. The late 5th and early 4th millennium cal BC correspond to the Middle Neolithic in Belgium, Middle Neolithic II in the French chronology, Middle Neolithic B in the Netherlands, the Early Neolithic in Britain and Ireland, and *Jungneolithikum* in Germany.

[2] *Chasséen septentrional* in French.

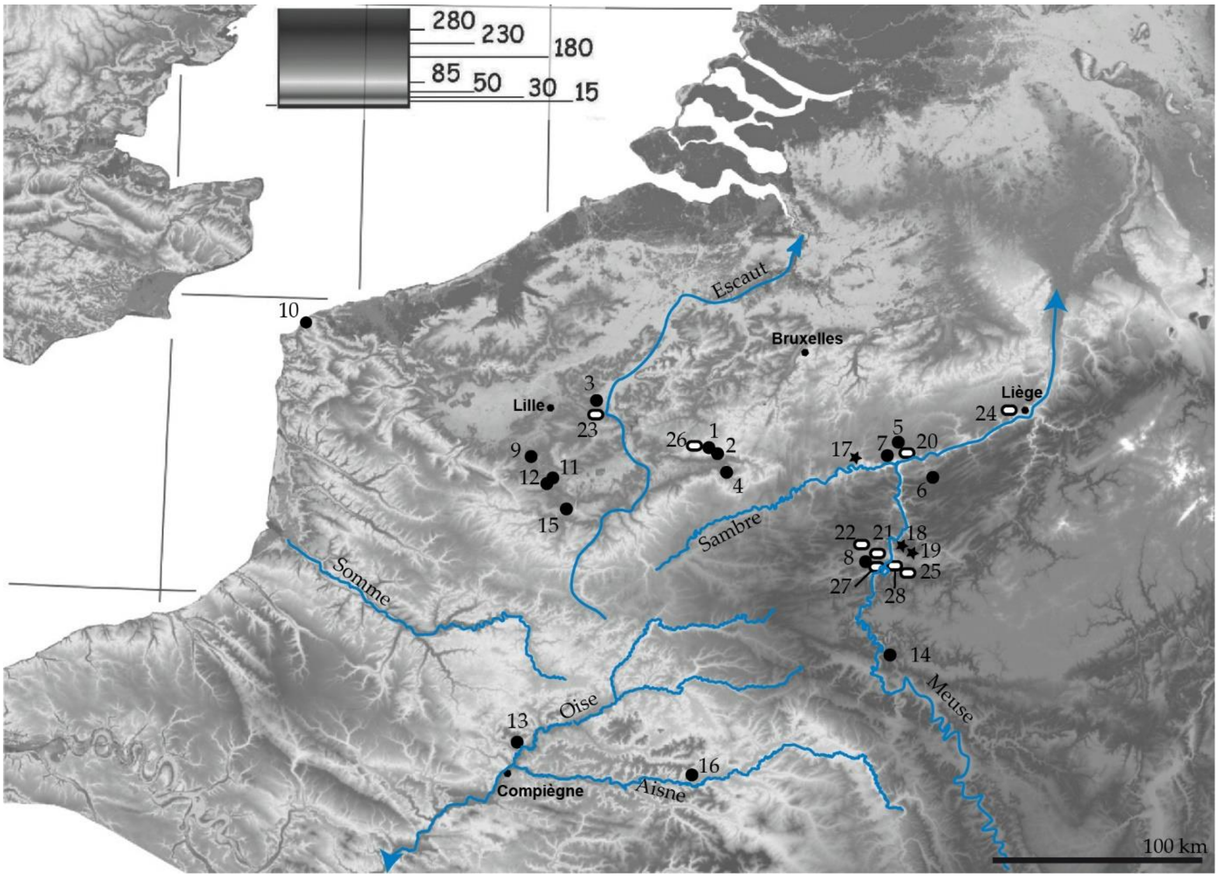

Fig. 1. Relief map (see the grey shades scale) locating: a) Fluorite occurrences in Neolithic sites. 1: Neufvilles; 2: Thieusies; 3: Spiere; 4: Petit-Spiennes; 5: Landenne; 6: Pont-de-Bonne; 7: Namur; 8: Olloy-sur-Viroin (in Belgium); 9: Carvin; 10: Escalles; 11: Lauwin-Planque-1; 12: Lauwin-Planque-2; 13: Passel; 14: Mairy; 15: Lécluse, and 16: Pontavert (in France); b) Fluorite from Upper Palaeolithic sites: 17: Spy cave (Jemeppe-sur-Sambre); 18: Trou Magrite cave (Dinant); 19: Trou de Chaleux cave (Houyet) and c) reference geological samples from Belgian and French geological deposits: 20: Seilles; 21: Gimnée; 22: Doische; 23: Foisches; 24: Chercq; 25: Chokier; 26: Lavaux-Sainte-Anne; 27: Neufvilles; 28: Sclayn. Infography by I. Praud.

The Neolithic fluorites were compared to Upper Palaeolithic (mainly Magdalenian) fluorites originating from the caves of Spy, Chaleux and Trou Magrite (Goemaere et al., 2013). All these caves formed in Visean limestones from the Namur and Dinant synclines (Fig. 1).

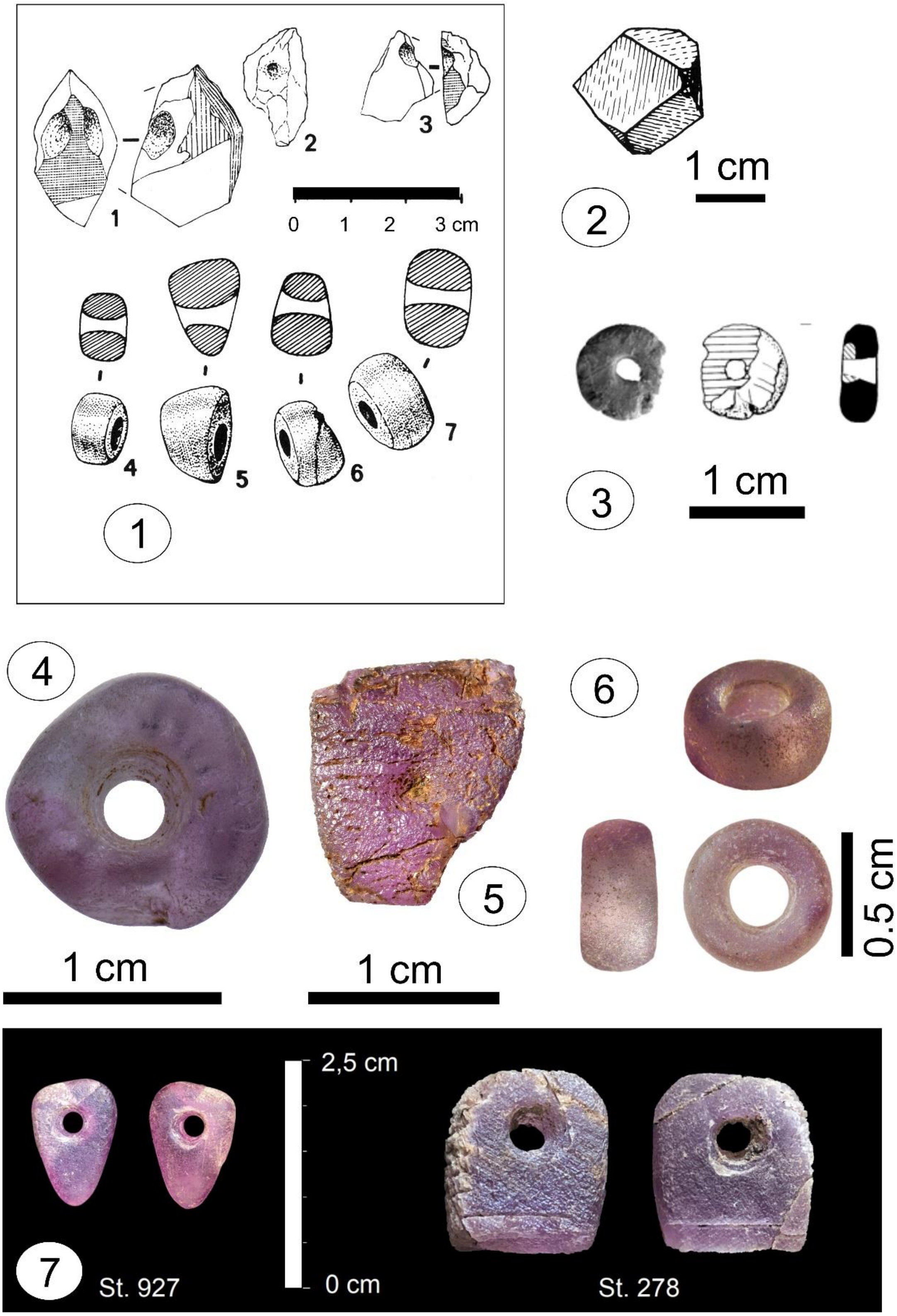

Fig. 2. A sample of pearls and fragments of archaeological fluorite described and analysed in this paper. 1) Thieusies (Vermeersch et al., 1990); 2) Neufvilles (De Heinzelin et al., 1977, p. 97, Fig. 43, n° 9); 3) Spiere (Vanmontfort et al., 2001/2002, p. 55); 4) Namur (D. Bosquet, AWaP); 5) Olloy-sur-Viroin (P. Cattelain, CEDARC-Musée du Malgré-Tout); 6) Mairy (Fourny and Van Assche, 2020), and 7) Passel (N. Cayol, Inrap).

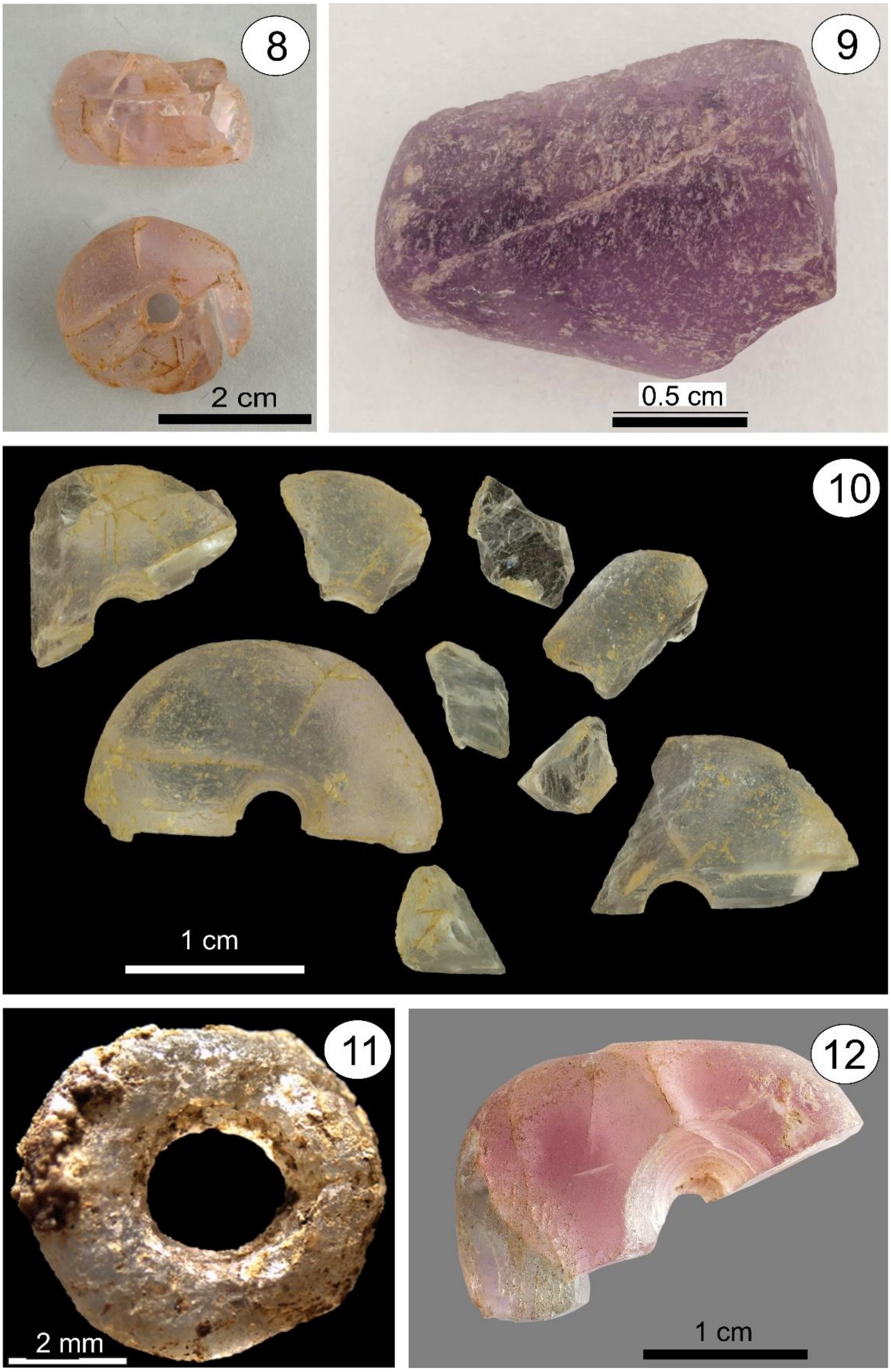

Fig. 3. A sample of pearls and fragments of archaeological fluorite described and analysed in this paper: 8) Lauwin-Planque “Zac” (E. Leroy-Langelin), after restoration; 9) Pont-de-Bonne (E. Delye); 10) Lauwin-Planque “Zac” before restoration (F. Bostyn, INRAP and UParis 1; Photo and Infography by É. Dewamme, RBINS); 11) Escalles (I. Praud); 12) Lauwin-Planque “Rue J Cartier” (D. Bossut, INRAP).

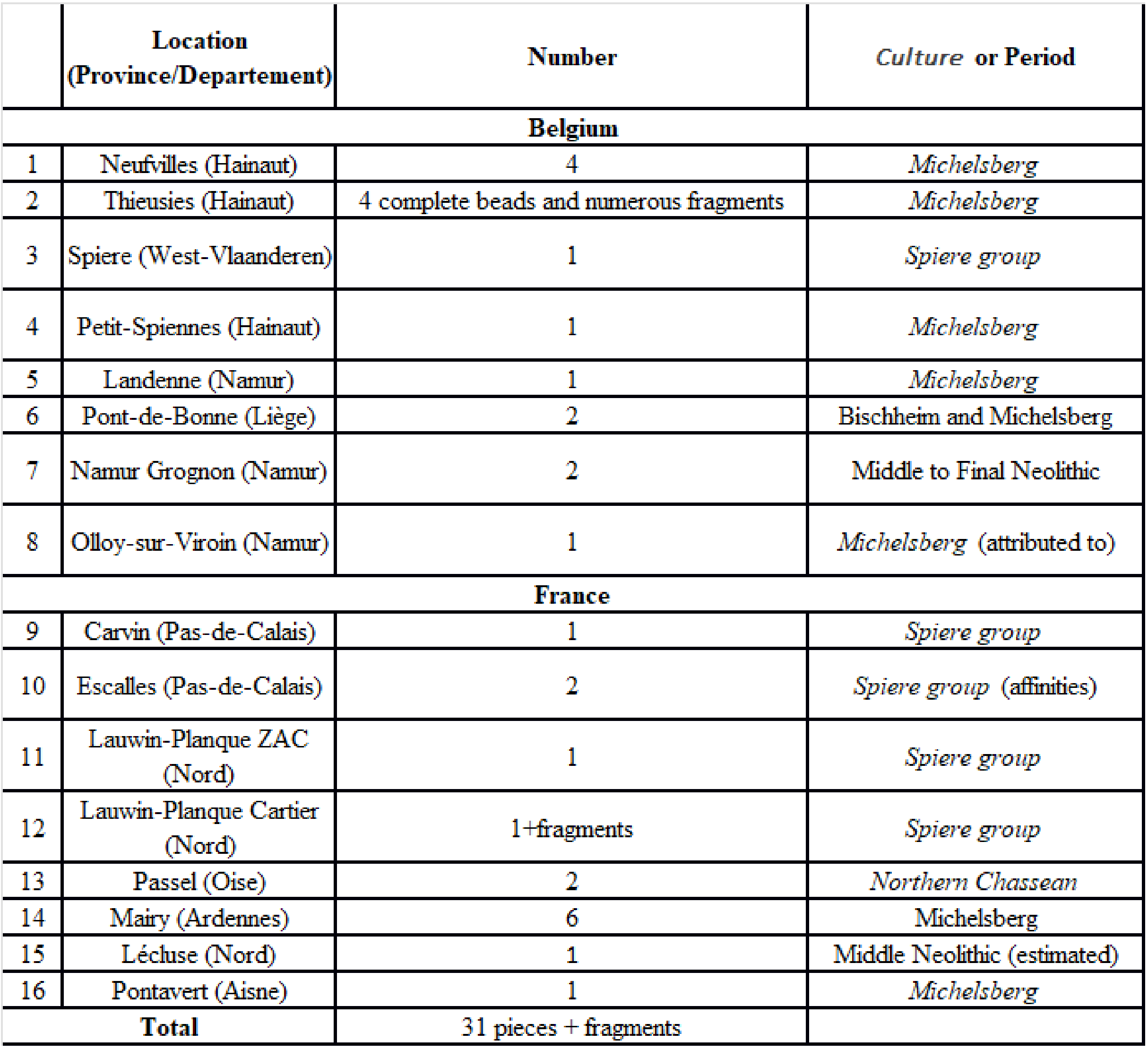

	Location (Province/Departement)	Number	*Culture* or Period
		Belgium	
1	Neufvilles (Hainaut)	4	*Michelsberg*
2	Thieusies (Hainaut)	4 complete beads and numerous fragments	*Michelsberg*
3	Spiere (West-Vlaanderen)	1	*Spiere group*
4	Petit-Spiennes (Hainaut)	1	*Michelsberg*
5	Landenne (Namur)	1	*Michelsberg*
6	Pont-de-Bonne (Liège)	2	Bischheim and Michelsberg
7	Namur Grognon (Namur)	2	Middle to Final Neolithic
8	Olloy-sur-Viroin (Namur)	1	*Michelsberg* (attributed to)
		France	
9	Carvin (Pas-de-Calais)	1	*Spiere group*
10	Escalles (Pas-de-Calais)	2	*Spiere group* (affinities)
11	Lauwin-Planque ZAC (Nord)	1	*Spiere group*
12	Lauwin-Planque Cartier (Nord)	1+fragments	*Spiere group*
13	Passel (Oise)	2	*Northern Chassean*
14	Mairy (Ardennes)	6	Michelsberg
15	Léchuse (Nord)	1	Middle Neolithic (estimated)
16	Pontavert (Aisne)	1	*Michelsberg*
Total		31 pieces + fragments	

Table 1. Dating of the layers in which analysed fluorites were recovered.

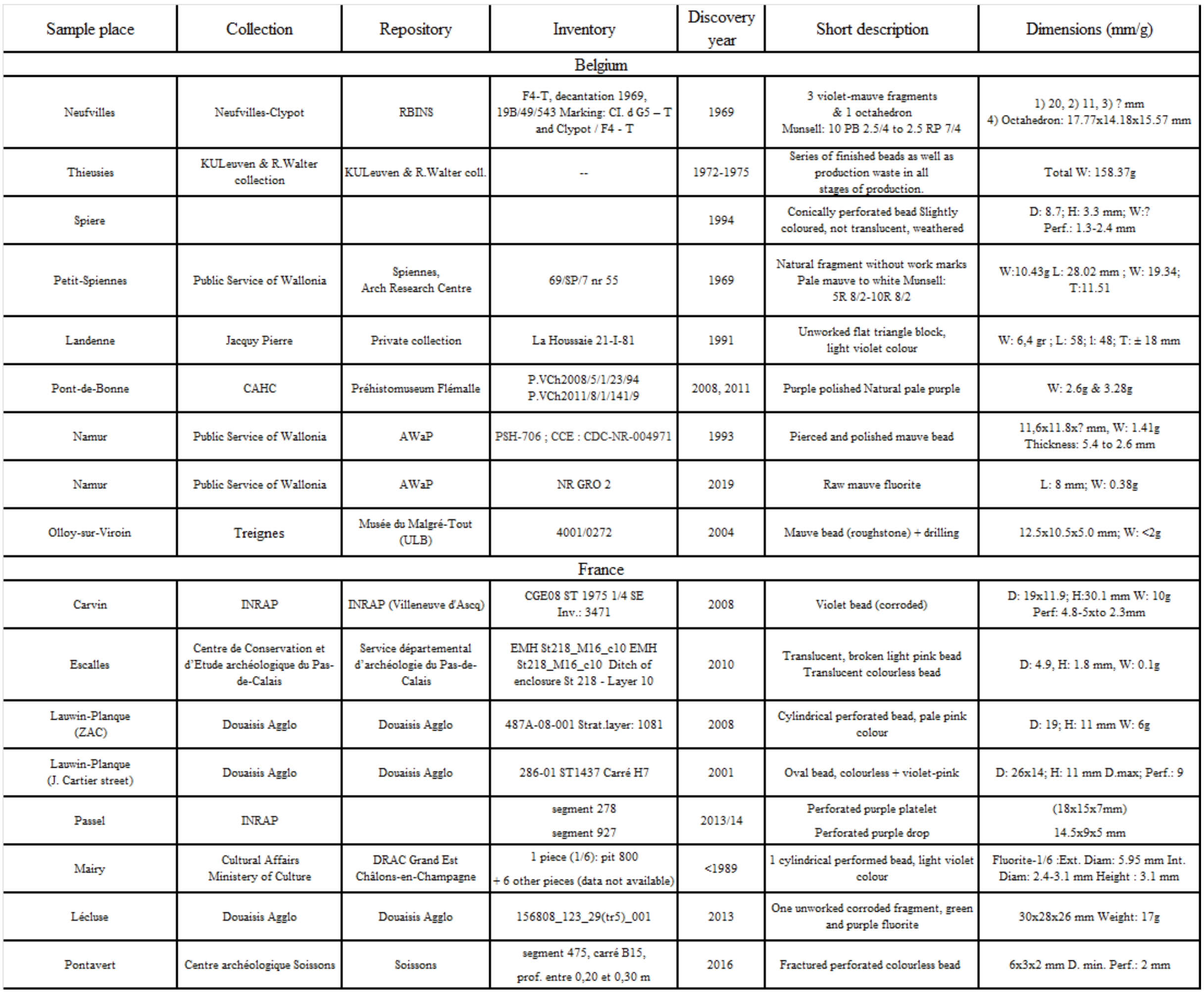

Sample place	Collection	Repository	Inventory	Discovery year	Short description	Dimensions (mm/g)
Belgium						
Neufvilles	Neufvilles-Clypot	RBINS	F4-T, decantation 1969, 19B/49/543 Marking: CI. d G5 – T and Clypot / F4 - T	1969	3 violet-mauve fragments & 1 octahedron Munsell: 10 PB 2.5/4 to 2.5 RP 7/4	1) 20, 2) 11, 3) ? mm 4) Octahedron: 17.77x14.18x15.57 mm
Thieusies	KULeuven & R.Walter collection	KULeuven & R.Walter coll.	--	1972-1975	Series of finished beads as well as production waste in all stages of production.	Total W: 158.37g
Spiere				1994	Conically perforated bead Slightly coloured, not translucent, weathered	D: 8.7; H: 3.3 mm; W:? Perf.: 1.3-2.4 mm
Petit-Spiennes	Public Service of Wallonia	Spiennes, Arch Research Centre	69/SP/7 nr 55	1969	Natural fragment without work marks Pale mauve to white Munsell: 5R 8/2-10R 8/2	W:10.43g L: 28.02 mm ; W: 19.34; T:11.51
Landenne	Jacquy Pierre	Private collection	La Houssaie 21-I-81	1991	Unworked flat triangle block, light violet colour	W: 6,4 gr ; L: 58; l: 48; T: ± 18 mm
Pont-de-Bonne	CAHC	Préhistomuseum Flémalle	P.VCh2008/5/1/23/94 P.VCh2011/8/1/141/9	2008, 2011	Purple polished Natural pale purple	W: 2.6g & 3.28g
Namur	Public Service of Wallonia	AWaP	PSH-706 ; CCE : CDC-NR-004971	1993	Pierced and polished mauve bead	11,6x11.8x? mm, W: 1.41g Thickness: 5.4 to 2.6 mm
Namur	Public Service of Wallonia	AWaP	NR GRO 2	2019	Raw mauve fluorite	L: 8 mm; W: 0.38g
Olloy-sur-Viroin	Treignes	Musée du Malgré-Tout (ULB)	4001/0272	2004	Mauve bead (roughstone) + drilling	12.5x10.5x5.0 mm; W: <2g
France						
Carvin	INRAP	INRAP (Villeneuve d'Ascq)	CGE08 ST 1975 1/4 SE Inv.: 3471	2008	Violet bead (corroded)	D: 19x11.9; H:30.1 mm W: 10g Perf: 4.8-5xto 2.3mm
Escalles	Centre de Conservation et d'Etude archéologique du Pas-de-Calais	Service départemental d'archéologie du Pas-de-Calais	EMH St218_M16_c10 EMH St218_M16_c10 Ditch of enclosure St 218 - Layer 10	2010	Translucent, broken light pink bead Translucent colourless bead	D: 4.9, H: 1.8 mm, W: 0.1g
Lauwin-Planque (ZAC)	Douaisis Agglo	Douaisis Agglo	487A-08-001 Strat.layer: 1081	2008	Cylindrical perforated bead, pale pink colour	D: 19; H: 11 mm W: 6g
Lauwin-Planque (J. Cartier street)	Douaisis Agglo	Douaisis Agglo	286-01 ST1437 Carré H7	2001	Oval bead, colourless + violet-pink	D: 26x14; H: 11 mm D.max; Perf.: 9
Passel	INRAP		segment 278 segment 927	2013/14	Perforated purple platelet Perforated purple drop	(18x15x7mm) 14.5x9x5 mm
Mairy	Cultural Affairs Ministery of Culture	DRAC Grand Est Châlons-en-Champagne	1 piece (1/6): pit 800 + 6 other pieces (data not available)	<1989	1 cylindrical performed bead, light violet colour	Fluorite-1/6 :Ext. Diam: 5.95 mm Int. Diam: 2.4-3.1 mm Height : 3.1 mm
Lécluse	Douaisis Agglo	Douaisis Agglo	156808_123_29(tr5)_001	2013	One unworked corroded fragment, green and purple fluorite	30x28x26 mm Weight: 17g
Pontavert	Centre archéologique Soissons	Soissons	segment 475, carré B15, prof. entre 0,20 et 0,30 m	2016	Fractured perforated colourless bead	6x3x2 mm D. min. Perf.: 2 mm

Table 2. Overview of the analysed archaeological fluorite fragments. D: bead diameter (mm); L: length (mm); l: width; H: height (mm); W: weight (g). AWaP: Agence wallonne du Patrimoine; Douaisis Agglo: Communauté d'Agglomération du Douaisis - Direction de l'Archéologie Préventive; INRAP: Institut National de Recherches Archéologiques Préventives; RBINS: Royal Belgian Institute of Natural Sciences.

3.2 The geological material

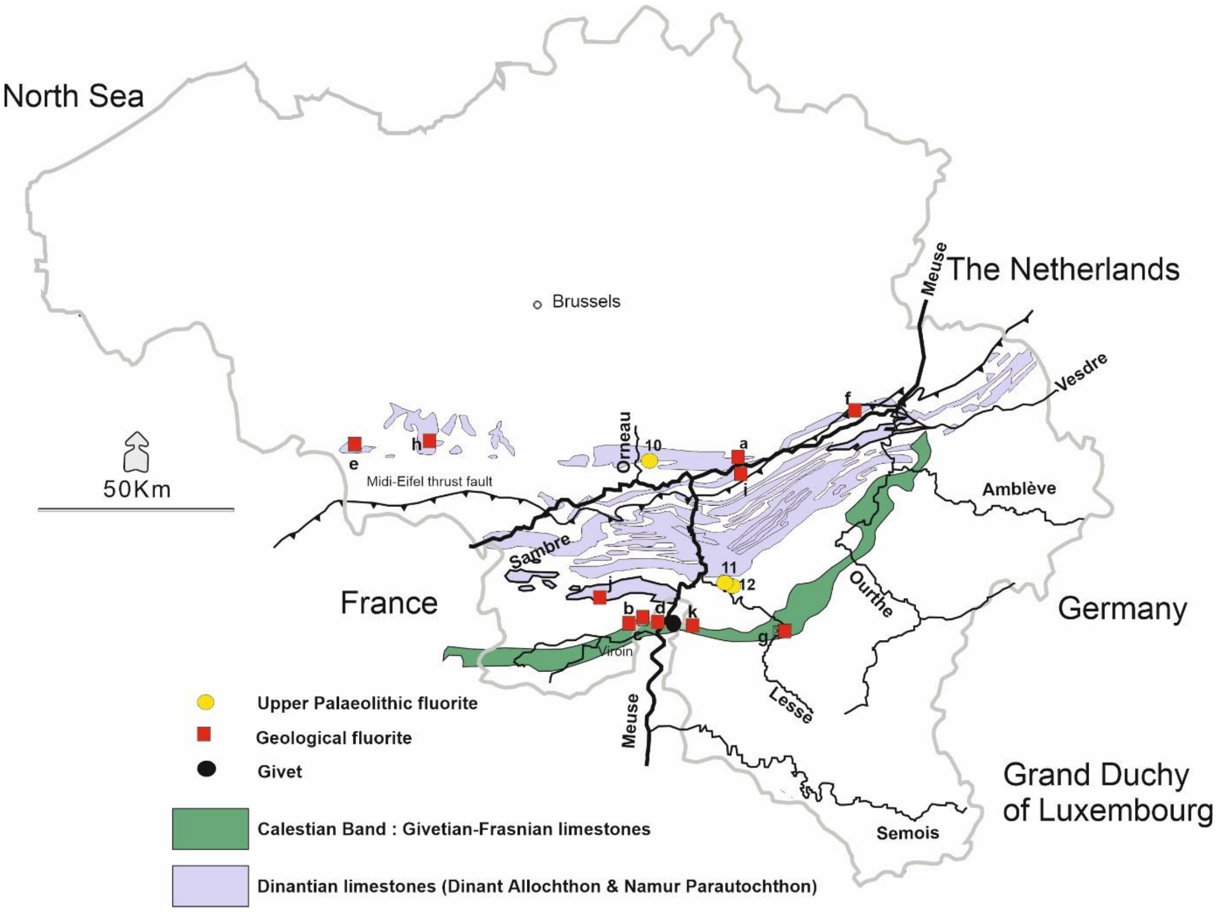

Fig. 4. Simplified geological map of Belgium showing the main limestone units and location of three caves with Upper Palaeolithic fluorite occurrences (yellow circles) and some geological outcrops (red squares). 10: Spy cave; 11: Trou Magritte cave ; 12: Chaleux cave; a : Seilles ; b : Gimnée, c : Doische ; d : Foisches, e : Chercq ; f : Chokier ; g : Lavaux-Sainte-Anne ; h : Neufvilles ; i : Sclayn ; j : Villers-en-Fagne and k : Rancennes.

In our study area, magmatic rocks are rare while metamorphic rocks (greenschist facies) are restricted to a limited surface in the Palaeozoic basement (Lower Palaeozoic and Lower Devonian) in the Ardennes. Fluorite has not been found in these series. Fluorite is mainly associated with Devonian (Givetian and Frasnian) and Dinantian (Tournaisian and Visean) limestones and dolostones (Fig. 4). Traces of fluorite are known in terrigenous Silesian rocks. These rocks, folded and faulted during the Variscan orogeny, belong to the Brabant Parautochthon (previously known as the Namur syncline) and the northern part of the Ardennes Allochthon (formerly called the Dinant and the Verviers synclines). Fluorite is totally absent in the Mesozoic and Cenozoic covers. Geological analysed samples are reported in Supplementary Information 1.

Fluorite occurrences in Belgium and Northern France (Nord Department, Hauts-de-France Region), are described by Baele (1994, 1998), Goemaere et al. (2013), and Swialkowski (2020). This mineral often occurs as small millimetre-sized grains dispersed in rocks, concentrated in stratification planes, or as small crystals located in geodes. Due to their inadequate crystal size and wide dispersion in host rock, these occurrences were unlikely to have been raw material sources in prehistory. Industrial extraction of limestones during the last two centuries has strongly modified the landscape, and has brought mineral samples to public and private collections. Only small-sized crystals of blue, colourless and violet fluorite were found in two active open quarries of Givetian limestones in the Avesnois (Nord Department, Hauts-de-France region) in Glageon (Groupement des carrières de l'Avesnois - groupe Eiffage), and at Wallers-en-Fagne (Swialkowski, 2020; Evlard and Swialkowski, 2020).

Significant amounts of fluorite are associated with silicified Givetian limestones in the natural region called the 'La Calestienne' (Dinant syncline) outcropping between Givet (French Ardennes) and Han-sur-Lesse (Belgian Famenne). Massive fluorite is restricted to the Givet area (Doische, Foisches, Gimnée, Rancennes), on both sides of the Franco-Belgian border. Fluorite only occurs in the fossiliferous silicified limestone of the Moulin Boreux and the Fort Hulobiet Members (Fromelennes Formation, Givetian). Fluorite seams, ranging between a few cm to 3 dm thick are disposed in broad subvertical fractures (Calembert and Van Leckwijk, 1942). Purple fluorite dominates over white, green and blue. In some places, unaltered beds of limestone contain some dispersed crystals of fluorite, which pass downstream to a layer of residual clay, sifted of more or less bulky fluorite masses. Fluorite was mined (restricted to hundreds of tons) in small, open pits and short galleries for a short time during the 20th century. Mining and collectors have drastically changed the original landscape. Numerous quarries extract the Dinantian limestones for ornamental stones, (do)lime and aggregates. Fluorite is found in all quarries, but only in small amounts and as small-sized crystals or formless grains.

The open Visean limestone quarry (Brabant Parautochthon) of Seilles (Andenne) is exceptional due to the occurrence of large pockets and metric veins of fluorite with a large range of colours. Numerous pieces show remarkable corroded surfaces, amplified along cleavage planes, due to acid leaching after Fe-Pb-Zn sulfide weathering. The quality of fluorite from Seilles enabled the production of faceted gemstones (Goemaere and Philippo, 2010; Goemaere et al., 2016). The rapid expansion of the quarry has destroyed this exceptional occurrence and the exact spatial relations between mineral and host rocks are at present poorly understood. We do not know if during prehistory the upper parts of the fluorite veins were visible at the surface or covered by sediments. Large amounts of fluorite from Seilles are present in the RBINS collection.

To conclude, the geographic area of occurrence of sufficiently large blocks of fluorite to produce ornaments is more restricted than the area where fluorite artefacts have been recovered. Fluorite thus must have been exported from its area of origin, especially towards the west.

3.3. Methods

Analytical methods used in this study are the same as those published in Goemaere et al. (2013). This allows an optimal comparison between geological samples and archaeological fluorites from Neolithic and Palaeolithic sites. The fluorites were carefully cleaved, hand-picked and observed under a binocular microscope to select the purest fragments of crystals. Fifty-four fluorite samples were analysed by Laser Ablation ICP-MS (23 Neolithic fluorites, 5 Palaeolithic fluorites and 26 geological fluorites, of which 19 were previously published in

Goemaere et al., 2013) and Sr-isotopic geochemistry methods. Sr-isotopic ratios were measured using a six-collector FINNIGAN MAT 262 TIMS (KU Leuven) and a NEPTUNE MC-ICP-MS with six Faraday cups (U. Gent). REE analyses were performed at the Field Museum of Natural History, Chicago, USA. With the exception of samples PDB1-3, all samples were analysed between 2008 and 2014 using a Varian Quadrupole ICP-MS (Elliot et al., 2004). Samples PDB1-3 were analysed in 2017 using a newer Thermo ICAP Q ICP-MS. Calibration protocols were identical across the analyses and are reported in Goemaere et al. (2013).

4. Analytical results

4.1. Results of the Multivariate Analysis

Geochemical data acquired by LA-ICP-MS chemical analysis both on archaeological (Belgian Upper Palaeolithic and Neolithic) and geological fluorites are given in Supplementary Information 2. For the multivariate analysis, the data were processed using the additive log-ratio transformation (alr) to comply with the relative nature of the geochemical data and to deal with the closure effect (Aitchison, 1986; Buxeda i Garrigós, 1999; Greenacre, 2018). A Kruskal-Wallis ANOVA was performed to identify the ratios allowing the best discriminations between the geological environments studied, and a Principal Component Analysis (PCA) was performed on the selected variables. Varimax rotation was applied to maximize the sum of the variance of the squared loadings. The aim was to make stronger associations between the factors and the most meaningful variables in order to achieve a better interpretation of results (Reimann et al., 2002). The data transformation was performed using CoDaPack software v. 2.01 and the Rotate PCA (RPCA) and the Kruskal Wallis ANOVA tests were performed using Xlstat software 2020 1.1 (Addinsoft, France).

The Kruskal-Wallis test was performed on all the elements measured in the 27 geological samples and normalised to the calculated CaF_2 content. The results show that B, Na, Al, Si, Ti, V, Co, Ni, Rb, Zr, Sb, Ba, U, and all the light rare earth elements (LREEs: La, Ce, Pr, Nd and Sm) are able to discriminate between fluorites from the Visean limestone and from the Calestian Band, with p-values < 0.05. These 19 elements have been selected for the RPCA. Because the heavy rare earth element (HREE) content of the archaeological samples can also provide useful information about their provenance, the nine HREEs have been summed and added as a 20th variable. The RPCA was first applied to the geological samples only. Then, archaeological samples were added as supplementary observations. Therefore, the construction of the Rotated Principal Components (RPCs) is only dependant on the composition of the geological samples.

After the Varimax rotation, the first two RPCs explain approximately 78% of the total variance of the database (Supplementary Information 3). All selected major and trace elements ratios are positively correlated with RPC1. The LREEs and the sum of the HREEs are strongly correlated with RPC2. As expected, there is a strong positive correlation between the LREEs, but the sum of the HREEs is only moderately correlated with the LREEs.

The fluorites from the Visean limestones and the Givetian silicified limestone are discriminated on the RPC1 - RPC2 plot (Fig. 5A). The geological samples from the Visean limestones originating from Seilles can be divided into three groups: group 1 is made of eight samples of different colours; group 2 includes the three green or pale green fluorite samples BRS022, BRS024 and BRS027; group 3 comprises the samples JGF005, JGF006 and JGF007. The other samples occurring in the Visean limestone collected outside of Seilles are scattered on the right side of the plot. With the exception of the sample from Sclayn, they are all located outside of the groups containing Seilles samples. The large variation in the data from the multicoloured fluorite vein of Seilles indicates the absence of a clear geochemical signature for a single site and the difficulty of discriminating between different sources of Dinantian fluorite.

The geological samples from the Calestian Band are scattered on the left side of the plot. The mauve samples from Doische, Gimnée, Rancennes, and Foisches have similar coordinates on RPC1, but they are dispersed on RPC2. It is worth noting that these four sites are located very near to one another. Moreover, the same pattern can be observed for the three samples from Han-sur-Lesse, Lavaux-Sainte-Anne and Ave-et-Auffe, three sites also separated by less than 10 km. Results based on this small set of fluorite samples from the Calestian Band seem to show that proximity between sites is reflected by the coordinates on RPC1. Therefore, the ratios for the major and trace elements contributing to RPC1 can potentially provide relevant information about the geographical location of sources.

The 27 archaeological samples are divided in three main groups on the RPC1-RPC2 plot (Fig. 5B). Group 1 includes eight Neolithic samples from different sites. Their scattered position on the right side of the plot reflects the heterogeneity of their major and trace element contents, and their relative homogeneity for the proportion of REEs. The samples from this group are relatively close to some geological samples from the Visean limestone from the Seilles quarry, but their position reflects a higher content of major and trace elements. Group 2 consists of seven Neolithic samples from Thieusies and one sample from Lauwin-Planque. They are characterised by higher REE ratios than those in group 1. Group 3 includes four Upper Palaeolithic samples and three Neolithic samples: two from Pont-de-Bonne and one from Escalles - Mont-d'Hubert. This group is located amid the geological samples from the Calestian Band, reflecting similar compositions for the elements selected in the RPCA. Three Neolithic samples from Thieusies and a single Neolithic sample from La Houssaie (Landenne) are outside of the main identified groups of archaeological samples. Because of their low REEs ratios, they are clearly associated with geological samples from the Visean limestone.

Results of the multivariate analysis show the similarity of elemental compositions of fluorites from Upper Palaeolithic sites with geological samples from the Calestian Band. The composition of fluorites from the Neolithic sites is more heterogeneous and could reflect a variation in the source of raw materials. Most of the Neolithic samples have an affinity with the chemical composition of fluorite from the Visean limestones. Two Neolithic samples from Pont-de-Bonne and one from Escalles-Mont-d'Hubert, on the contrary, are located close to the Upper Palaeolithic samples. This proximity could reveal a common origin from the Calestian Band.

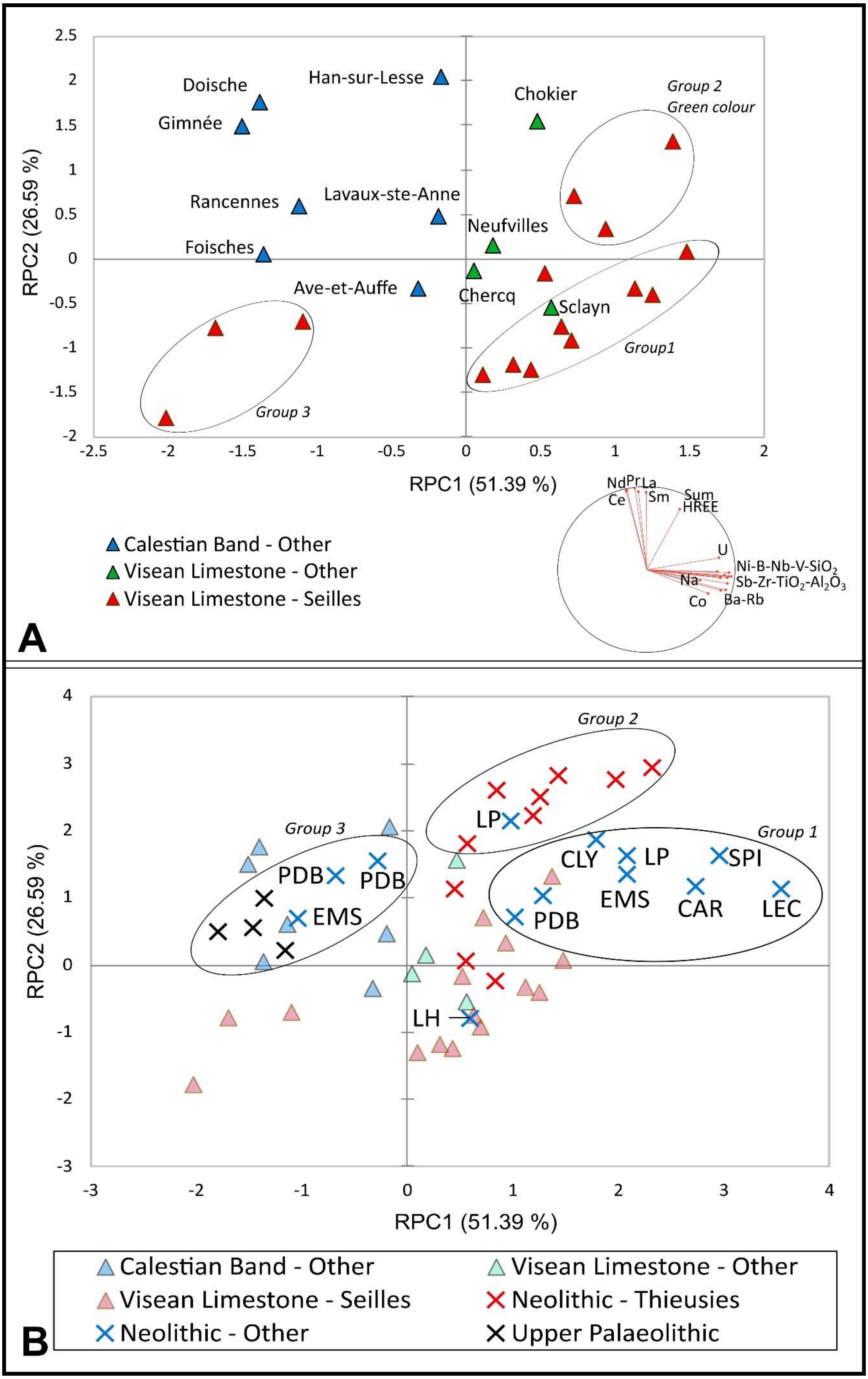
RPC2 (26.59 %)
RPC1 (51.39 %)
2.5
2
1.5
1
0.5
0
-0.5
-1
-1.5
-2
-2.5
-2
-1.5
-1
-0.5
0
0.5
1
1.5
2
Doische
Gimnée
Han-sur-Lesse
Chokier
Group 2
Green colour
Rancennes
Lavaux-ste-Anne
Neufvilles
Foisches
Ave-et-Auffe
Chercq
Sclayn
Group1
Group 3
Nd
Pr
La
Ce
Sm
Sum
HREE
U
Ni-B-Nb-V-SiO$_2$
Na
Sb-Zr-TiO$_2$-Al$_2$O$_3$
Co
Ba-Rb
▲ Calestian Band - Other
▲ Visean Limestone - Other
▲ Visean Limestone - Seilles
A
RPC2 (26.59 %)
RPC1 (51.39 %)
4
3
2
1
0
-1
-2
-3
-3
-2
-1
0
1
2
3
4
Group 2
Group 3
Group 1
LP
CLY
LP
SPI
PDB
PDB
EMS
CAR
LEC
EMS
PDB
LH
△ Calestian Band - Other
△ Visean Limestone - Other
△ Visean Limestone - Seilles
✕ Neolithic - Thieusies
✕ Neolithic - Other
✕ Upper Palaeolithic
B

Fig. 5. A) PCA plot displaying geological fluorite samples. B) PCA plot displaying archaeological and geological samples. CAR: Carvin; CLY: Clypot (Neufvilles); EMS: Escalles - Mont-d'Hubert; LEC: Lécluse, LH: La Houssaie (Landenne); LP: Lauwin-Planque (ZAC and Cartier); PDB: Pont-de-Bonne, SPI: Spiennes. Infography by T. Delbey.

4.2. REE results

Geochemistry of rare earth elements is widely used in ore geology in general and in the study of fluorite ore, and Goemaere et al. (2013) use REEs profiles to trace the source of Upper Palaeolithic fluorite. Chemical results show a wide variation in the concentration of any particular REE in archaeological fluorites, as well as total REE content (11 to 310 ppm). The range of the least abundant REE, Tm, is 0.285-5.414 ppm and the range of the most abundant REE, Nd, is 0.55-58.1 ppm. The lighter REEs, La to Gd, are not always more abundant than the heavier REEs, Tb to Yb (Fig. 6). Green coloured fluorites are richer in REEs, but no other relationship has been established with other colours, possibly due to the small size of our dataset. This is slightly in disagreement with Naldrett et al. (1987), who find no relation between the absolute (nor the enrichment or depletion of a particular REE) REE content and the colour of any particular sample.

Very low REE concentrations are found in three fluorites from Thieusies, one from Pont-de-Bonne, and one from La Houssaie. Fractionation in fluorites is highly variable, with La/Yb ratios varying between 0.5 and 44. REE distributions for all Neolithic fluorites are shown in Fig. 6. The REE distributions of the archaeological fluorites show three different types of chondrite-normalised patterns, mainly (except one sample from Thieusies, with peculiarly low REEs) with a negative but variable (strong to low) Eu anomaly. Positive and negative Ce anomalies are noted. The type-1 profile shows enrichment in LREEs, especially for Nd, followed by a rapid decrease in the content of other REEs. This is the case for seven samples from Thieusies, two from Pont-de-Bonne and one from Lauwin-Planque. Samples from Neufvilles, Petit-Spiennes, Escalles (n=2), Carvin, Lécluse, and a single sample from Lauwin-Planque show flatter profiles with lower LREE/HREE ratios.

The type-2 pattern is flat and markedly depleted in REEs, with a very low LREE/HREE ratio near or below one. This is the case for the fluorites from La Houssaie and one sample from Pont-de-Bonne. The type-3 profile is represented by a single sample from Thieusies. Its shape shows a hump with highest values between Nd and Er, with depletion in very light REEs (La, Ce and Pr). Baele et al. (2011, 2019) show that fluorite bulk REE analysis "may be biased by compositional heterogeneity in crystals". These authors report "a systematic REE partitioning in cubo-dodecahedral fluorite crystals from Belgium using cathodoluminescence spectral imaging and LA-ICP-MS analysis". The light REEs are markedly enriched, and heavy REEs depleted in the |110| sector relative to the |100| sector. The partition coefficient K |110|/|100| is >10 for LREEs and <1 for HREEs. Figure 7 confirms the conclusions of Baele et al. (2011, 2020), especially regarding the very large distribution of values in Seilles fluorite coming from a unique vein. Very contrasting REE patterns and ratios are thus recorded from the same crystal. The fact that the partition coefficient gradually decreases from La to Gd may be associated with the influence of the ionic radius of the REE^{3+} substituting for Ca^{2+} in the fluorite lattice. The REE concentration can vary during crystal growth but without modification of the pattern shape. Partitioning of REEs as a function of the sector analysed makes REE patterns problematic for comparison of archaeological samples and source raw material. This likely explains why three fluorites (of type 2 pattern) from Thieusies and the fluorite from La Houssaie are classified in a special group in the multivariate analysis. Consequently, it could be reasonable to consider that all fluorites from Thieusies come from the same source. Profiles (Fig. 6) established for Upper Palaeolithic sources look like the type-2 Neolithic fluorite patterns, with low concentrations of LREEs and depleted HREEs (fluorite from Neufvilles, Carvin, Petit-Spiennes, Escalles (n=2) and Lauwin-Planque-1), but they differ in having a weak Ce positive anomaly and higher values of HREEs having paired atomic numbers. REE patterns of geological fluorites show shapes like the types-1 and 2 described above, with a possible fourth type comprised of a single sample from Villers-en-Fagne, which is enriched in HREEs. Consequently, we cannot allocate Neolithic fluorites to specific Dinantian or Devonian sources using REE patterns alone. Were artefacts prepared from fluorite masses without crystal faces or from large crystals? In all cases, all natural faces disappeared during the production process. Only the cleavage planes {111} can be observed. Future analyses will have to take in account the crystallographic orientation of artefacts (parallel to the {110} cube faces) by relying on the orientation of the cleavage planes, which are often recognizable. It could be useful to multiply the measures from the core to the outside to follow variations in fluid composition.

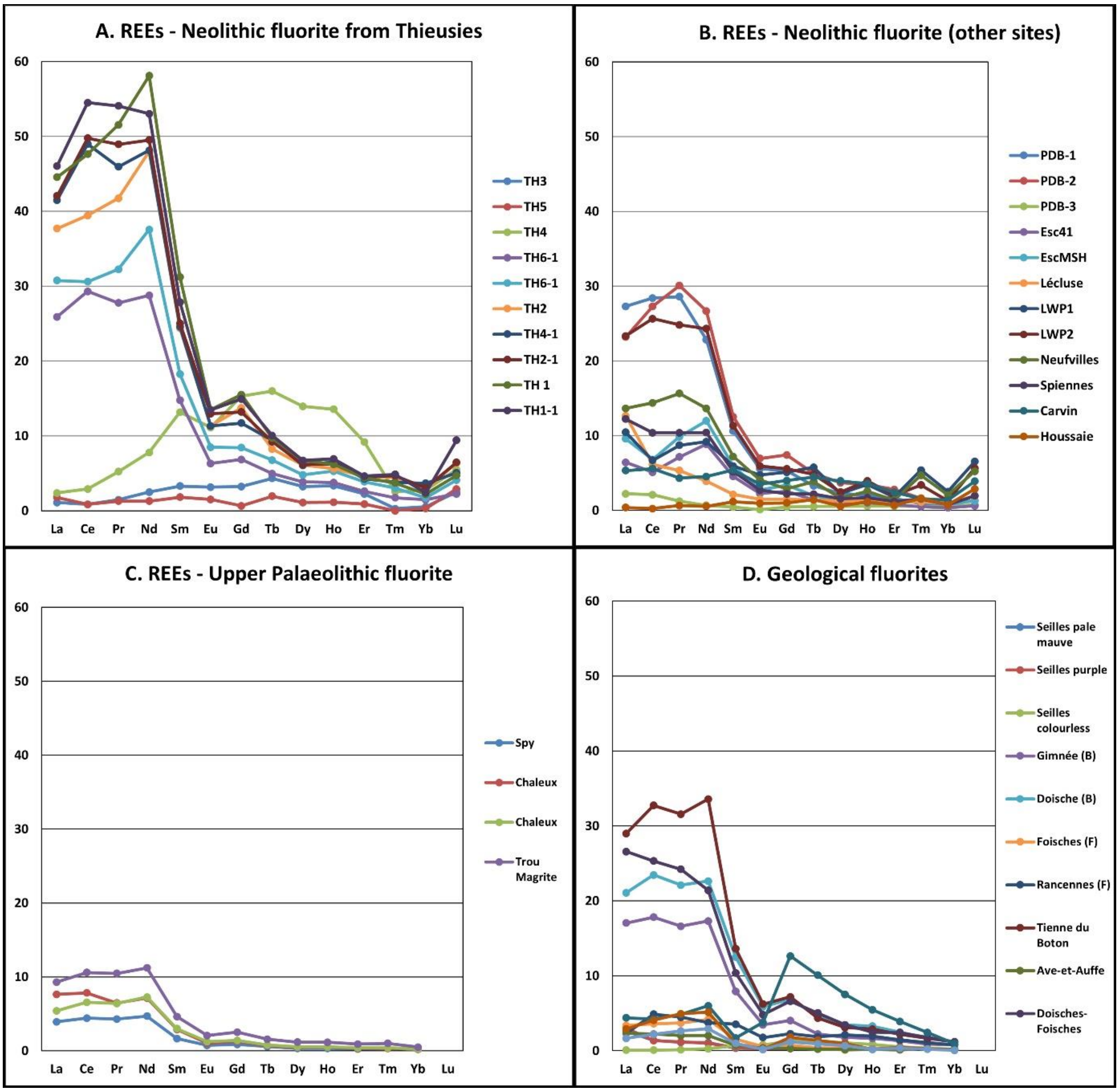

Fig. 6. Chondrite-normalised REE contents in archaeological fluorites. a) Fluorite from Thieusies; b) Fluorites from other Neolithic sites; c) Upper Palaeolithic fluorites; d) Geological fluorites. Values normalised after Sun and MacDonough (1989).

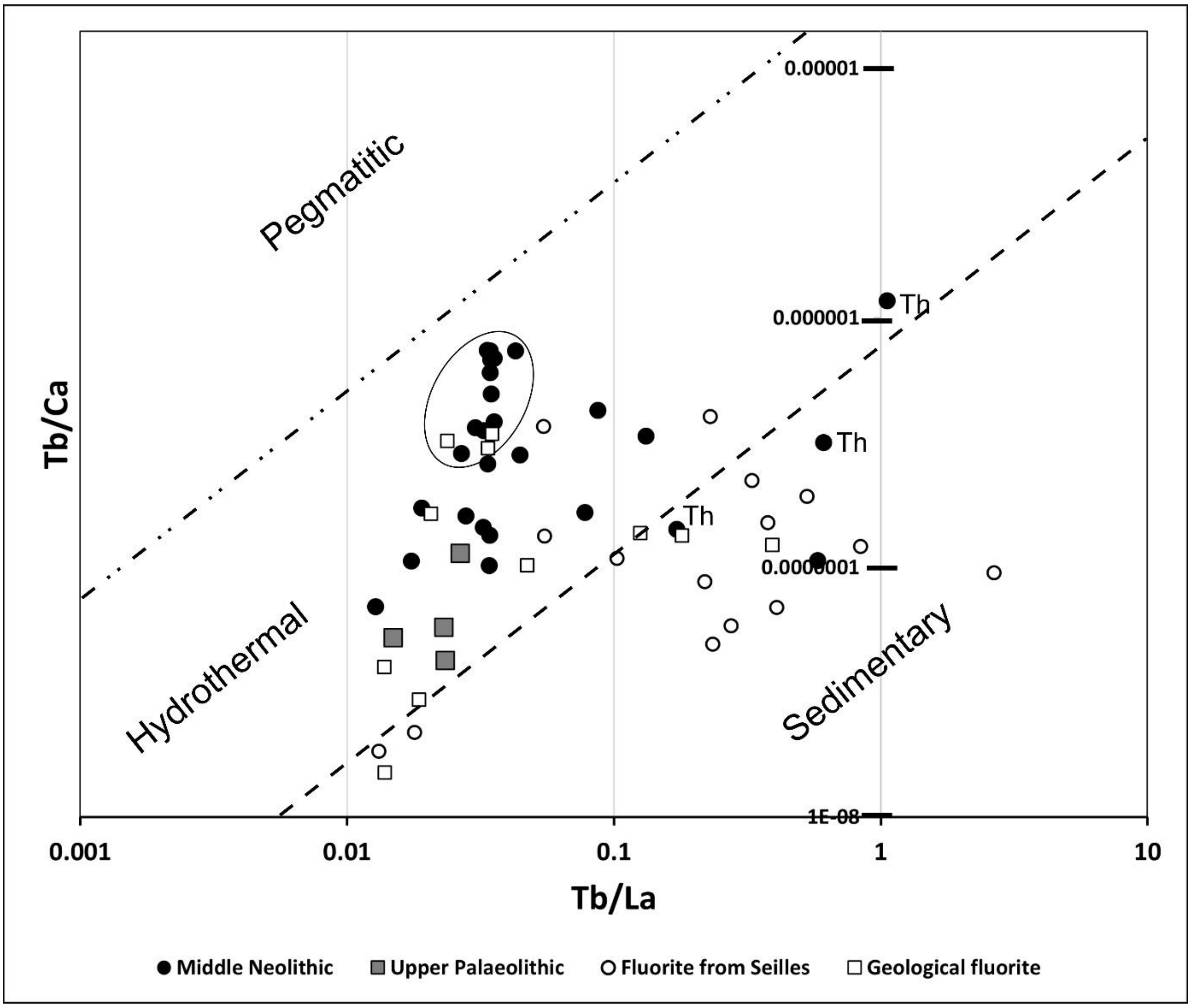

Fig. 7. Tb/La-Tb/Ca diagram (log scales) after Baele et al. (2011). Ellipse: majority of fluorite samples from Thieusies, Th: additional samples from Thieusies. Most fluorites are in the hydrothermal domain, while fluorites from the vein of Seilles show a very large distribution indicative of different analysed sectors.

4.3. Sr-isotopic results

Sr isotopes ($^{87}Sr/^{86}Sr$) have proven to be a useful indicator of water-rock interaction as a geochronological tool and as a tracer for groundwater movement and the origin of salinity. They are also used in archaeological science to trace raw materials for artefact production, e.g. glass and metal (Degryse and Schneider, 2008; Degryse et al., 2007) or ceramics (Li et al., 2006). Goemaere et al. (2013) apply this method to trace the origin of fluorite excavated in caves occupied during the Upper Palaeolithic.

Sr and REEs are able to substitute for Ca in fluorite, given their similar ionic radii. ^{87}Sr is the decay product of ^{87}Rb, hence the older the parent rock is, the higher the $^{87}Sr/^{86}Sr$ ratio will be (depending on the original amount of ^{87}Rb). Since different geological deposits were formed at different periods in the earth's history, specific Sr-isotopic signatures will be observed which can be used to identify geological origin. When REEs are used in provenance studies, Eu-anomalies are the most important feature: these anomalies in sedimentary rocks reflect the dispersion of the rocks within the earth's crust.

The Sr content of the analysed fluorites is low (12-248 ppm), as are Rb contents, which are typically below 0.8 ppm, except in fluorite from Lécluse (5.3 ppm), Petit-Spiennes (2.1 ppm), and Escalles (1.5 ppm) (Supplementary Information 2). With an Rb/Sr ratio below 0.1%, the correction of in-situ ^{87}Rb decay is thus negligible for these fluorites and the measured ^{87}Sr/^{86}Sr ratio may be considered as representative of the initial ratio. Analytical results from this study, data on four previously analysed fluorites by Demaiffe and Dejonghe (1990), together with data published by Goemaere et al. (2013), are shown in Table 3. Sr isotopic values obtained on Upper Palaeolithic archaeological fluorites have similar values (0.70838-0.70853) and can be associated with geological fluorites from the Givetian (0.70841-0.70855) of the Calestian Band, mainly the two proximal locations of Foisches (France) and Gimnée (Belgium). Only six pieces of Neolithic fluorite were analysed, five from Thieusies and one from Spiere, due to the destructive nature of this method and the very restricted number of pieces (Table 3, Fig. 8), limiting conclusions to two sites. The Sr-isotopic ratios from both Thieusies and Spiere are between 0.70974 and 0.71287, in the same range as Dinantian fluorite and two fluorites from Neufvilles. Sr-isotopic ratios of Neolithic fluorite are significantly higher than Givetian fluorite and Upper Palaeolithic fluorite. None of the Neolithic fluorites (as well as Upper Palaeolithic fluorites) have marine Sr-signatures, the probable reason for the relatively wide range of values, due to the variation in the composition of mineralizing fluids.

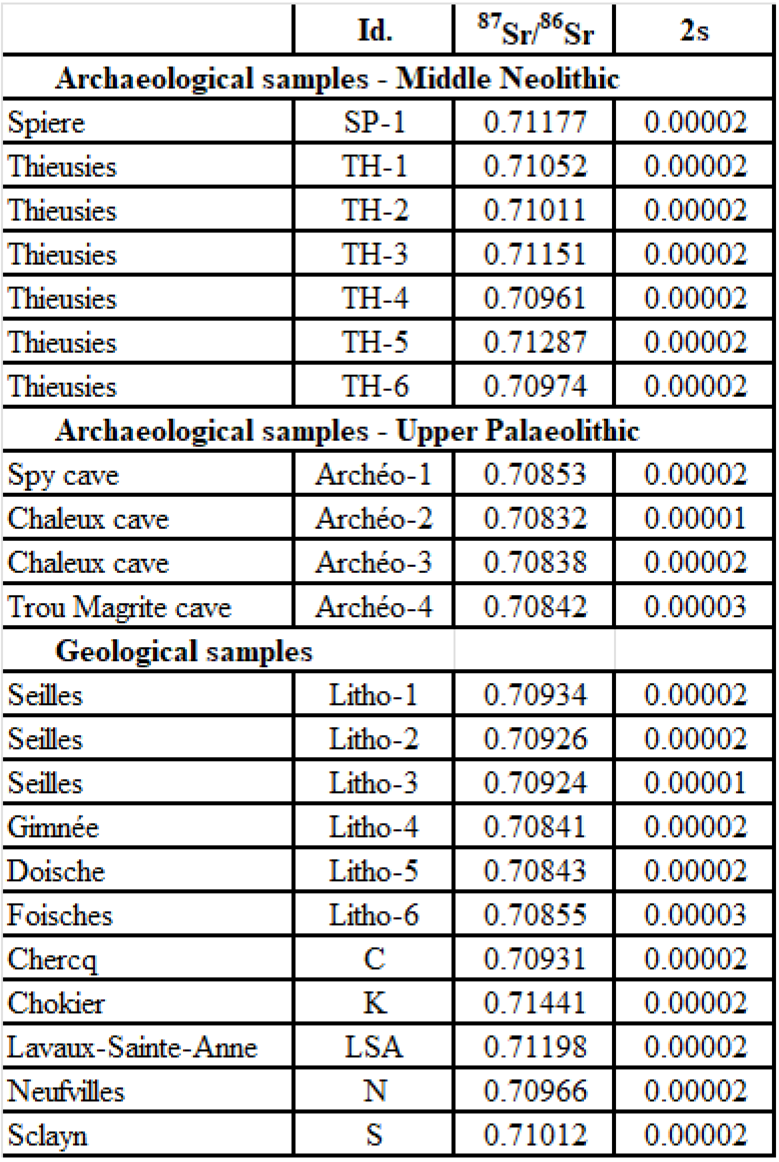

	Id.	^{87}Sr/^{86}Sr	2s
Archaeological samples - Middle Neolithic			
Spiere	SP-1	0.71177	0.00002
Thieusies	TH-1	0.71052	0.00002
Thieusies	TH-2	0.71011	0.00002
Thieusies	TH-3	0.71151	0.00002
Thieusies	TH-4	0.70961	0.00002
Thieusies	TH-5	0.71287	0.00002
Thieusies	TH-6	0.70974	0.00002
Archaeological samples - Upper Palaeolithic			
Spy cave	Archéo-1	0.70853	0.00002
Chaleux cave	Archéo-2	0.70832	0.00001
Chaleux cave	Archéo-3	0.70838	0.00002
Trou Magrite cave	Archéo-4	0.70842	0.00003
Geological samples			
Seilles	Litho-1	0.70934	0.00002
Seilles	Litho-2	0.70926	0.00002
Seilles	Litho-3	0.70924	0.00001
Gimnée	Litho-4	0.70841	0.00002
Doische	Litho-5	0.70843	0.00002
Foisches	Litho-6	0.70855	0.00003
Chercq	C	0.70931	0.00002
Chokier	K	0.71441	0.00002
Lavaux-Sainte-Anne	LSA	0.71198	0.00002
Neufvilles	N	0.70966	0.00002
Sclayn	S	0.71012	0.00002

Table 3. ^{87}Sr/^{86}Sr ratios performed on archaeological and geological fluorites.

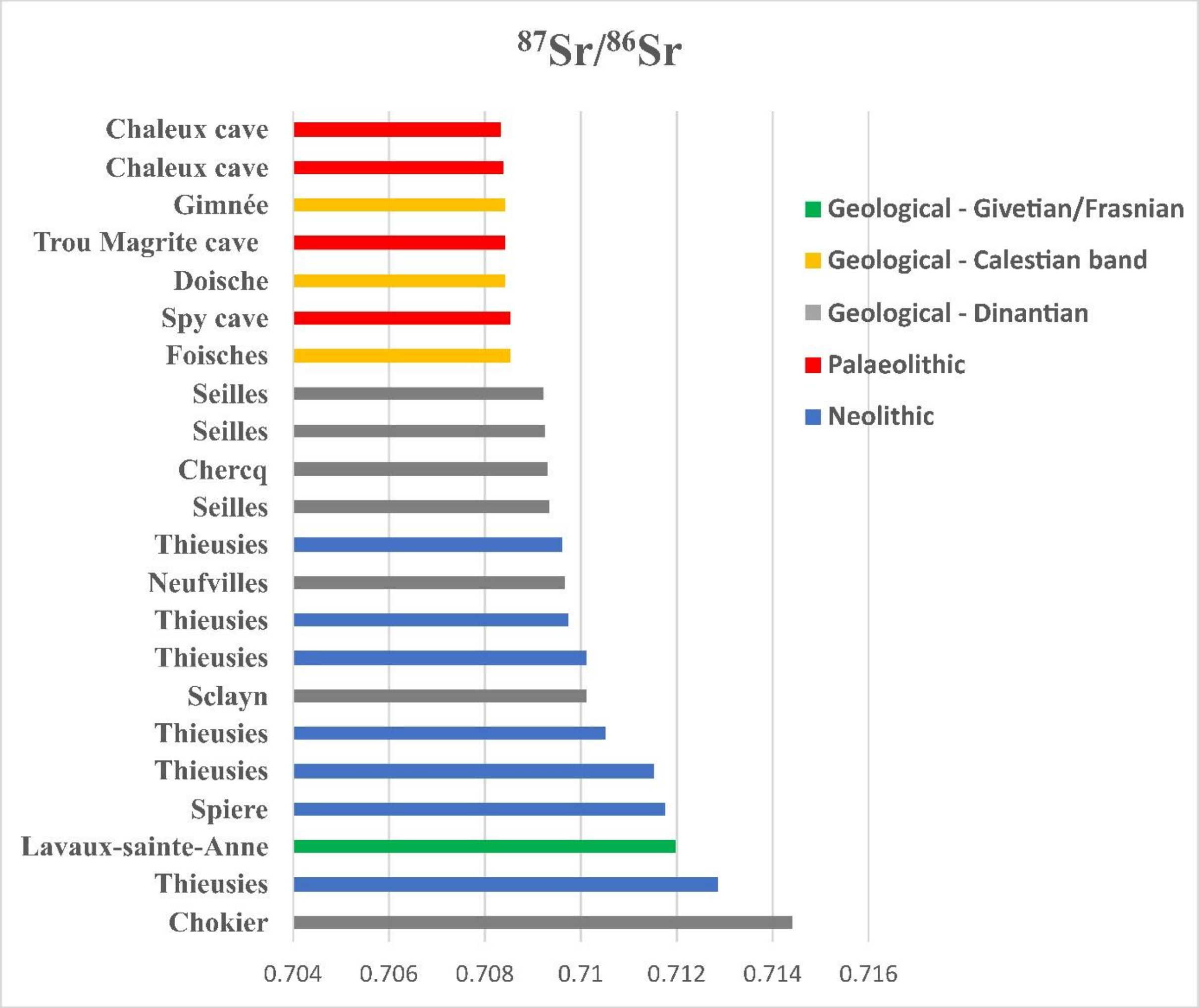

Fig. 8. Graph plotting measured Sr-isotopic ratios. See Table 3 to find the correspondence with the Id. and the precise Sr isotopic values. Infography by É. Goemaere.

5. Discussion

5.1. Critical evaluation of the analytical methods

The first limitation of our study is the rarity and the small size of the fluorite artefacts in the archaeological record, drastically diminishing their availability for destructive analyses, in particular for small and rare shaped and polished beads and pearls. It is no longer necessary to demonstrate the possibility of geochemical analyses by LA-ICP-MS to trace the sources of archaeological artefacts. However, Baele et al. (2011, 2019, p. 151) show that “crystal growth may exert a dramatic influence on REE incorporation in fluorite. The effect may be so strong that REE patterns from a single crystal can look very different, except for Ce and Eu anomalies, which seem unaffected. Such compositional heterogeneity should be taken into consideration when conducting bulk or in-situ analysis of trace elements in fluorite, as well as when interpreting the resulting REE data”. As a consequence, statistical data processing will also be drastically affected. Registration of fluorescence emission spectra of fluorites could be attempted to find specific signatures, but these spectra are driven by REEs and must be conducted as a function of the crystal orientation; this method is limited in practice if destructive preparation of the sample is required. Furthermore, fluorite is sensitive to corrosion in both geological deposits and archaeological layers. This corrosion progresses along the easy cleavage planes with incorporation in depth of a colloidal to micrometric mineralogical fraction (Fig. 9a). Finally, hydrothermal fluorite is rich in fluid inclusions (Fig. 9b), sometimes of multiple generations and trapped during the crystallization process and used to determine the composition and temperature of these fluids. Until now, no attempt has been made to measure these parameters to track down sources of raw material. Impurities and fluid inclusions are limiting agents for several methods, such as XRD and XRF. Although Sr isotopic measurement is a useful technique to differentiate geological occurrences that is not impacted by these issues, this method requires destructive sampling, which constitutes an impassable obstacle in the case of very small fluorite artefacts.

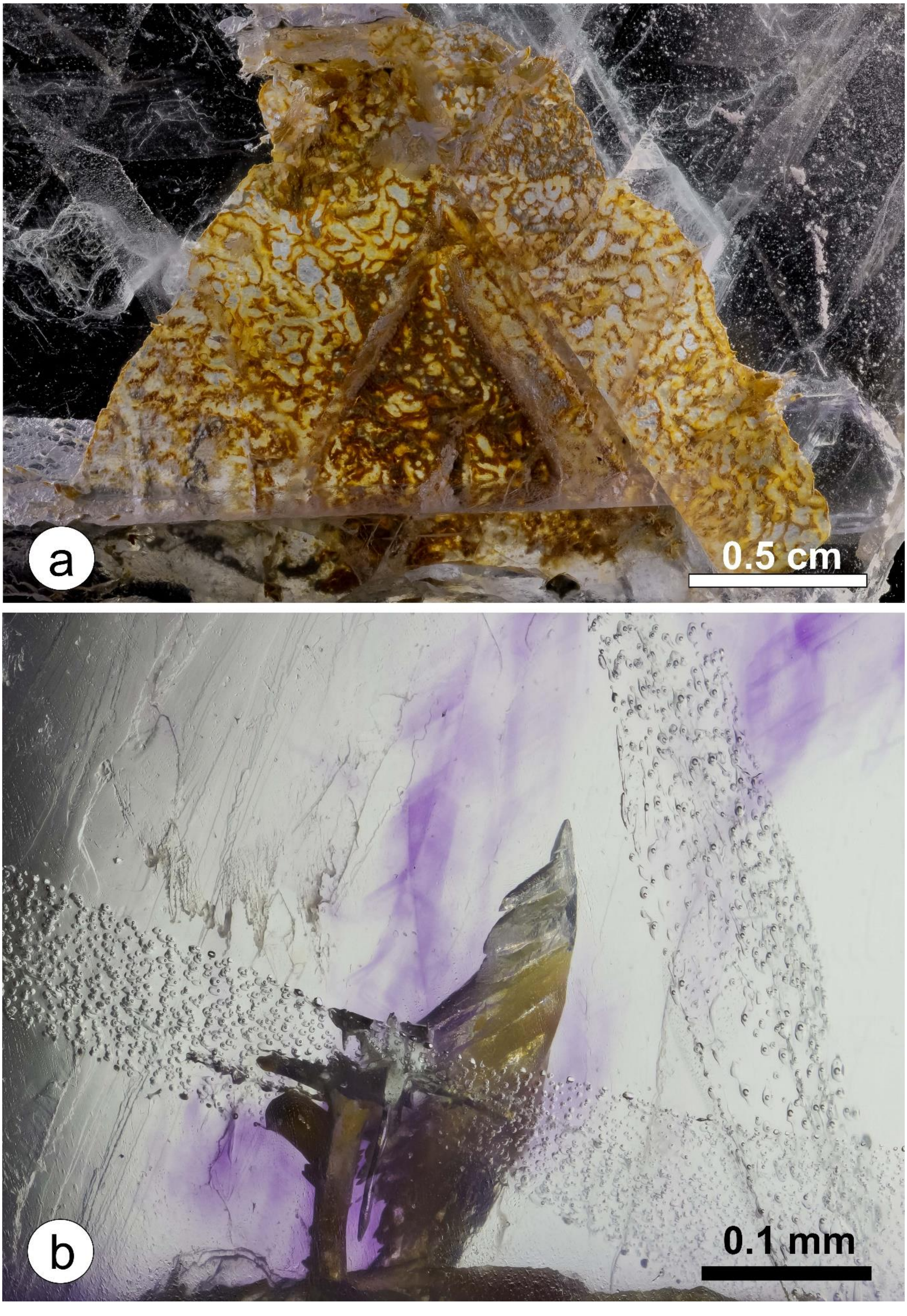

Fig. 9. 9a) Infilling of colloidal clays (yellow-brown colour) along a cleavage plane in a fluorite from Seilles. Note the traces of the {111} cleavage network. Rik Dillen collection.

Photo by Eddy Van Der Meersche. 9b) Two oblique sectors rich in two-phase fluid inclusions. Corrosion channel lined with yellowish colloids in a bicolour fluorite from Seilles. RBINS collection. Photo by Eddy Van der Meersche.

5.2. Sourcing of the Middle Neolithic fluorite

Despite these limitations, some conclusions can be drawn with respect to sourcing of the analysed fluorites. None of the studied Neolithic fluorites have a marine Sr-signature, all derived from hydrothermal fluids and are consistent with Mississippi valley-type Pb-Zn-F-Ba deposits. When comparing the Neolithic samples with four Upper Palaeolithic samples, one can notice a clear difference. The Upper Palaeolithic samples all have $^{87}Sr/^{86}Sr$ ratios near to 0.708, which is consistent with marine Sr-isotopic ratios dated to the Givetian and allows the identification of the source of the fluorite in the Givetian silicified limestones of the Calestian Band in the Givet area (Goemaere et al., 2016). The Sr-isotopic ratio of the Neolithic samples from Thieusies and Spiere almost all exceed 0.710, which excludes an origin from the same source as all Upper Palaeolithic samples. Sr-isotopic ratios of the Neolithic fluorites cover a wide range that corresponds with a source in the Dinantian limestones. It should be noted that a single sample from the anticline (Devonian limestone “island” close to the Calestian Band) of the Bois du Roptai in Lavaux-Sainte-Anne, from the Devonian limestones beyond the Givet region, also falls within this range. More analyses are needed to identify the specific range of the Sr-isotopic ratios of the fluorites from these Devonian limestones.

The Neolithic samples display a large range of Sr isotopic values and range of colours. All identified signatures and colours, however, confirm a potential source from within the wider area of southern Belgium. Colours of fluorite beads found in the studied area cover the dominant colours of Belgian geological fluorites. Yellow fluorites, occurring in southern France, Spain, and Portugal, were not encountered.

Sr-isotopic ratios are only available for the objects from two sites. Additional analyses on fluorite artefacts from more sites are needed to confirm the distinction of this range from the signature of fluorite from the Givet area that was sourced during the Upper Palaeolithic. A wide range of signatures is also observed on the PCA graph of geological and archaeological fluorite samples. Contrary to the specific signature of the fluorites from the Calestian band near Givet from which the Palaeolithic objects were sourced, the Neolithic samples display a much wider spectrum that partially overlaps with the geological samples from the Calestian band, partially with those of the Visean limestones and partially extends beyond the sampled geological spectra. The data for fluorite from a single vein in the Visean limestones from Seilles, in any case shows the potential variation within fluorite from a single specific source. Despite this variation, the Calestian band fluorite from Givet is still identifiable and the sourcing of Palaeolithic fluorites demonstrated by Goemaere et al. (2016) can be confirmed. Due to the wide spectrum of signatures for Neolithic fluorites, we cannot decide between multiple sources or a single source with large variation. It is possible that during the Neolithic more fluorite sources were exploited than during the Palaeolithic (Givet and non-Givet area) and the potential sources are widespread and in several cases lay close to these Neolithic sites. Furthermore, no source of fluorite has been identified that covers the full spectrum of the archaeological samples. More sampling is required but no more archaeological fluorites are currently available.

Many Neolithic sites in Belgium are located near to or on Dinantian limestones/dolostones, potential sources of fluorite. Note that Dinantian limestones (north flank of the Brabant Parauchthon) outcrop in the valley near the Gué du Plantin (Neufvilles) archaeological site, but no fluorite veins were observed there during the two last centuries, only small-sized crystals in calcite veins. Limestones and dolostones were intensively mined since the Roman period in a large area from the present-day border with France to that with the Netherlands. Based on the Seilles spectrum on fig. 5 and the Dinantian spectrum on fig. 8, it cannot be excluded that the Thieusies objects/samples all come from a single source. The site of Olloy-sur-Viroin is located on the Calestian Band, which is well known for its fluorite content in some places. For this site, from which fluorite was not studied by archaeometric methods, it cannot be ruled out that raw material was locally collected. We hope new excavations will bring numerous fluorite fragments available for future (destructive) analyses to refine the search for sources of raw materials.

5.3. Archaeological implications

Most of the fluorite fragments and artefacts studied in this paper date to the Middle Neolithic period of the region during the late 5th and early 4th millennia BC. For half of the samples, this date is secured by the archaeological contexts in which the objects were found, and these contexts can be dated on the basis of radiocarbon dates or associated archaeological assemblages attributed to the Michelsberg Culture or Spiere group. A single site is attributed to the contemporaneous northern Chassean. In a number of other sites this Middle Neolithic association can be assumed with confidence because of the association with Michelsberg Culture artefact assemblages, even if those assemblages were found in secondary contexts or in surface assemblages mixed with more recent artefacts or radiocarbon dates. The cultural layer from the site of Namur "Grognon" in which fluorites were discovered contains material from Middle to Final Neolithic, and its precise chronologic attribution remains to be confirmed. The Michelsberg Culture and the northern Chassean are two of the main archaeological cultures in Western and Central Europe during the late 5th and early 4th millennium cal BC. At its largest extent, the Michelsberg Culture covered a region from the Seine River in the West to the Weser basin and Bavaria to the east (Jeunesse, 2010), but fluorite artefacts are only known from the western part of that area, corresponding to present day Belgium and Northern France. Not a single fluorite fragment is reported from numerous known Late and Final Neolithic funerary contexts in the study region, and only a single bead from a Bronze Age burial mound at Mol is known.

This near exclusive association with the Middle Neolithic of the region is remarkable. It contrasts with the situation in southwestern Europe, where the Late Neolithic and Copper Age are even characterised by an increase in finds of fluorite ornaments (Garrido-Cordero et al. 2021). There was apparently no preference for fluorite in the production of ornaments in northern France and Belgium after the middle of the 4th millennium, even if the raw material remained available regionally.

This coincides with the start of fluorite use in southwestern Europe, where fluorite ornaments are almost exclusively found as grave goods and generally associated with objects produced in (other) exotic materials. In the northern Belgian and Northern French group, on the other hand, not a single fluorite object has been found in the few known Middle Neolithic burial sites. All fluorite included in our dataset (and known for the region) was recovered from settlement contexts, and none of these are associated with exotic raw materials. Exotic raw materials are also absent from contemporaneous burial contexts in Northern France and Belgium (e.g. Colas et al. 2007; 2015), but occurs more commonly in southwestern Europe - considerations on the special meaning of fluorite because of its association with exotic objects in burial contexts elsewhere (cf. Garrido-Cordero et al. 2021) can thus not simply be transposed to the items found in the study region. That their presence on settlement sites is the result of accidental loss is rather unlikely, given their near absence in settlement sites of southern France or Iberia. Instead, they may well be related with and the result of a burial rite consisting of body exposure and disarticulation at or near settlement or enclosure sites, as has been suggested earlier on the basis of dispersed human remains at those sites (e.g. Thomas 1999, 43; Vanmontfort 2004, p. 227) and the general scarcity of burial sites.

Our sourcing data shows that most sites where fluorite was found had access to that raw material regionally within distances of no greater than 20 km as the crow flies. Even if its translucent character and colouring most probably determined the special character of fluorite, it does not seem to have been exchanged and distributed over great distances.

Three archaeological sites in Northern France, Escalles, Passel and Pontavert, are exceptions to this regional distribution. These sites are located at a greater distance from limestones and show the circulation of finished products, possibly from Belgium, over distances of c. 130 km, and at Escalles, over 250 km. The affinities in material culture of these sites, shown by the attribution of Escalles and Pontavert to the regional Spiere group or Michelsberg culture, suggest that fluorite exchange was an intra-community affair. For Passel, the only site where fluorite beads were found in a context attributed to an affiliated archaeological culture, the northern Chassean, the precise nature of contacts cannot be determined. However, even for Passel, the distance covered from the nearest location where fluorite could have been acquired is much shorter than the hundreds of kilometres claimed for fluorite in the Tagus estuary (Cardoso et al. 2012). It should be stressed that in the latter case, the most probable raw material source is located in the same river catchment (*ibid.*). It thus fits the regional character that typifies fluorite distribution in Europe (Garrido-Cordero et al. 2021). Despite the fairly restricted number of fluorite fragments, a wide variety in colour and most probably also in sources can be observed. This means that there was no particular search for specific colours and no specific fluorite source that was exploited, in contrast to the Palaeolithic period. Rather, the data fit with opportunistic and small-scale exploitation as was suggested by Garrido-Cordero et al. (2021). Together with the regional character of the sourcing and the absence of exotic raw materials in burial contexts, this supports the view that during the Middle Neolithic period, people turned to either perishable materials like tooth or locally available raw materials (Cauwe 1997; Hauzeur & Cauwe 2012). Cauwe (1997) links this change to societal changes and the importance of the collective within Middle Neolithic society of the region. If fluorite ornaments were used as an expression of identity, this only played out on a regional, and most probably intra-community level.

6. Conclusion

The measurement of Sr isotopes ratios is the best method for tracing the source of fluorite, while heterogeneous concentrations within single crystals mean that the interpretation of REEs curves must be used with caution. Results show that Neolithic fluorite originates from different local and regional sources, mainly the Dinantian limestones/dolostones of the Ardennes Allochthon, in contrast to the use of silicified Givetian limestones of the Calestian Band near Givet (France) during the Magdalenian.

Neolithic use of fluorite as a raw material for the production of ornaments is known from a large area in the western part of Europe, from present-day Belgium in the north to southern Spain and Portugal in the south. The number of fluorite objects is generally restricted and they almost always occur on sites with regional access to raw material. No large-scale exploitation, production and supraregional distribution of fluorite has been attested so far and an opportunistic exploitation is proposed. If it was used for the expression of identity, it was likely on an intra-community level. The use and deposition of Neolithic fluorite from the northern Middle Neolithic sites that were studied in this paper differs from that seen elsewhere in Western Europe. Fluorites in Northern France have been exclusively found on settlement sites, whereas elsewhere they are almost exclusively known from funerary contexts. This may be related to a burial rite consisting of body exposure and disarticulation.

Acknowledgements

The authors are grateful to Philippe Lavachery, Fanny Martin, and Nathalie Mees from the AWaP (at the time of excavations), René Walter, the scientists of the Cedarc/Musée du Malgré-Tout, Michel Fourny and Michel Van Assche for helping us in the search for fluorite archaeological finds in Belgium and Northern France, and É. Dewamme (photographer, RBINS). The authors kindly acknowledge the constructive criticism and helpful comments of three anonymous reviewers and the editors, which greatly contributed to improvement of this paper.

Funding

LA-ICP-MS analyses were partially funded by United States National Science Foundation grants BCS0320903 and BCS1531394.

Supplementary data

Supplementary data associated with this article can be found online at https://doi.org/10.1016/j.jasrep.2023.103980.

Declaration of Competing Interest

The authors declare that they have no known competing financial interests or personal relationships that could have appeared to influence the work reported in this paper.

References

Aitchison, J., 1986. The statistical analysis of compositional data. Springer.

Baele, J.-M., 1994. Étude des silicifications. Le cas des fagnolithes de l'Entre-Sambre-et-Meuse. Unpublished MA-thesis, Fac. Polytech. Mons.

Baele, J.-M., 1998. Reliques silicifiées et minéralisées de paléokarsts post-varisques sur le Dévonien en Belgique méridionale (Entre-Sambre-et-Meuse). Ann. Soc. Géol. Nord 6 (2), 127-133.

Baele, J.-M., Monin, L., Navez, J., André, L., 2011. Systematic REE partitioning in cubo-dodecahedral fluorite from Belgium revealed by cathodoluminescence spectral imaging and Laser Ablation-ICP-MS. In Broekmans, M.A.T.M. (Ed.), Proceedings of the 10th International Congress for Applied Mineralogy, Chap. 4, Springer Berlin Heidelberg, 23-30. https://doi.org/10.1007/978-3-642-27682-8_4

Baele, J.-M., Decrée, S., Rusk, B., 2019. Cathodoluminescence applied to ore geology and exploration. In: Decrée, S., Robb, L. (Eds), Ore Deposits: Origin, Exploration, and Exploitation, Geophysical Monograph 242, First Edition, Section 2: new methods for mineral exploration, chap. 6, 133-161.

Bailloud, G., Dauvois, M., Horemans, P., Nouel, A., Planchais, N., Poulain-Josien, T., Riquet, R., 1965. L'ossuaire néolithique d'Eteauville, (Eure-et-Loir). Bull. Soc. Préh. Fr., Etudes et travaux 62 (3), 576-648.

Barge, H., 1982. Les parures du Néolithique ancien au début de l'Age des métaux en Languedoc, CNRS.

Beex, G., Roossens, H., 1963. Drieperiodenheuvel met klokbekers te Mol. Archaeologia Belgica 72, 7-19.

Buxeda i Garrigós, J., 1999. Alteration and contamination of archaeological ceramics: The perturbation problem. J. Archaeol. Sci. 26(3), 295-313. https://doi.org/10.1006/jasc.1998.0390

Calembert, L., Van Leckwijk, W., 1942. Les gisements de fluorine belges et français du bord méridional du synclinorium de Dinant. Ann. Soc. Géol. Belg. 65, 64-75.

Cardoso, J.L., Domínguez, S., Martínez, J., 2012. Ocorrência de contas de fluorite no Neolítico Final e no Calcolítico da Estremadura (Portugal). Estudos Arqueológicos de Oeiras 19, 35-42.

Cauwe, N., 1997. De l'objet à la figuration. Limites de l'étude de la parure néolithique. Vie Archéologique 48, 15-24.

Colas, C., Manolakakis, L., Thevenet, C., Baillieu, M., Bonnardin, S., Dubouloz, J., Farruggia, J.-P., Maigrot, Y., Naze, Y., Robert, B., 2007. Le monument funéraire Michelsberg ancien de Beaurieux 'la Plaine' (Aisne). In Besse, M. (ed) Sociétés néolithiques. Des faits archéologiques aux fonctionnements socio-économiques. Actes du 27e colloque interrégional sur le Néolithique, Cahiers d'archéologie romande 108, Lausanne, 329-334.

Colas, C., Naze, Y., Thevenet, C., avec la collaboration de Gransar, F., 2015. Le site de Cuiry-lès-Chaudardes "Le Champ Tortu" (Aisne). Un village Michelsberg d'un nouveau type? Revue Archéologique de Picardie, 3/4, 229-248.

Degryse, P., Schneider, J., 2008. Pliny the Elder and Sr-Nd radiogenic isotopes: provenance determination of the mineral raw materials for Roman glass production. J. Archaeol. Sci. 35, 1993-2000. https://doi.org/10.1016/j.jas.2008.01.002

Degryse, P., Schneider, J., Kellens, N., Waelkens, M., Muchez, P., 2007. Tracing the resources of iron working at ancient Sagalassos (south-west Turkey): A combined lead and strontium isotope study on iron artefacts and ores. Archaeometry 49, 75-86.

De Heinzelin, J., Haesaerts, P., De Laet, S.J. avec la collaboration de Bastin, B., Czepiec, S., Gautier, A., Hulthén, B., Splingaer, M., Van Doorselaer, A. (1977). Le Gué du Plantin (Neufvilles, Hainaut), site néolithique et romain. Dissertationes archaeologicae Gandenses XVII, Bruges.

Demaiffe, D., Dejonghe, L., 1990. Géochimie isotopique du strontium des barytes, anhydrites, calcites et fluorites de Belgique. Ann. Soc. Géol. Belg. 113 (2), 231-240.

Elliot, S., Knowles, M., Kalinitchenko, I., 2004. A new direction in ICP-MS. Spectroscopy 19, 30-38.

Evlard, J., Swialkowski, M., 2020. La carrière de "Pierre bleue" de Wallers-en-Fagne, Nord. Le Règne Minéral, Hors-série XXV/XXVI, 142-154.

Fourny, M., Van Assche, M., 2020. Le site Micheldsberg de Mairy « Hautes Chanvières » (FR). Analyses carpologiques et palynologiques, passées et à venir. Notae Praehistoricae 40, 47-49.

Garrido-Cordero, J.A., Odriozola, C.P., Sousa, A.C., Gonçalves, V.S., 2020a. Fluorite and translucent beads in Iberian Late Prehistory. Materials and Manufacturing Processes 35 (13), 1424-1430. https://doi.org/10.1080/10426914.2020.1753069

Garrido-Cordero, J.A., Odriozola, C.P., Sousa, A.C., Gonçalves, V.S., Cardoso, J.L., 2020b. Distribution and consumption of fluorite and translucent beads in the Iberian Peninsula from the 6th to the 2nd millenia BC. Trabajos de Prehistoria 77 (2), 273-283. https://doi.org/10.3989/tp.2020.12256

Garrido-Cordero, J.A., Odriozola, C.P., Sousa, A.C., Gonçalves, V.S., Cardoso, J.L., 2021. Shine on your crazy diamond: symbolism and social use of fluorite ornaments in Iberia's late prehistory. J. Lith. Stud. 8 (1), 1-17. https://doi.org/10.2218/jls.3025

Gaydarska, B., Chapman, J., 2008. The aesthetics of colour and brilliance – or why were prehistoric persons interested in rocks, minerals, clays and pigments? In Kostov, R.I., Gaydarska, B., Gurova, M. (eds), Geoarchaeology and Archaeomineralogy. Proceedings International Conference, Sofia, 63-66.

Goemaere, E., Honings, J., Jungels, C., Golitko, M., Degryse, P., Schneider, J., 2013. Discerning geological and geographical sources of Belgian Upper Paleolithic fluorites by rare earth elements and Sr-isotopic geochemistry. J. Archaeol. Sci. 40, 2892-2901. https://doi.org/10.1016/j.jas.2013.02.029

Goemaere, E., Philippo S., 2010. La Fluorite de Seilles. In Terres, Pierres et Feu en Vallée Mosane. L´exploitation des ressources naturelles minérales de la commune d'Andenne, IRSNB, Bruxelles, 491-500.

Goemaere, E., Robert, A., Van der Meersche, E., Leduc, T., 2016. La fluorite de Seilles (Andenne, province de Liège, Belgique). Le Règne Minéral 129, 23-29.

Greenacre, M., 2018. Compositional data analysis in practice. CRC Press.

Hauzeur, A., Cauwe, N. 2012. La parure au Néolithique. In P. Cattelain, N. Bozet, and G. V. Di Stazio (eds.): La parure de Cro-Magnon à Clovis. Guides Archéologiques du Malgré-Tout, Éditions du CEDARC. Treignes, Belgique: 36-45.

Honings, J., Goemaere, E., Bostyn, F., Monchablon, C., Leroy-Langelin, E., Degryse, P., Golitko, M., Collet, H., Jadin, I., 2014. REE and Sr-isotopic geochemistry: tools to determine the geological and geographical origins of Neolithic fluorites. In: Scott, R.B., Braekmans, D., Carremans, M., Degryse, P. (Eds.), Proceedings 39th Intern. Symp. Archaeom. Centre for Archaeological Science, KU Leuven.

Jeunesse, C., 2010. Die Michelsberger Kultur. Jungsteinzeit im Umbruch. In: Lichter, C. (Ed.), Die "Michelsberger Kultur" und Mitteleuropa vor 6000 Jahren. Badisches Landesmuseum, Karlsruhe, 46-55.

Jungels C., Goemaere E., 2007. La fluorite: une matière première inhabituelle en Préhistoire. Notae Praehistoricae 27, 27-39.

Li, B.P., Zhao, J.X., Greig, A., Collerson, K.D., Feng, Y.X., Sun, X.M., Guo, M.S., Zhuo, Z.X., 2006. Characterisation of Chinese Tang sancai from Gongxian and Yaozhou kilns using ICP-MS trace element and TIMS Sr-Nd isotopic analysis. J. Archaeol. Sci. 33, 56-62. https://doi.org/10.1016/j.jas.2005.06.007

Magotra, R., Namga, S., Singh, P., Arora, N., Srivastava, P.K., 2017. A New Classification Scheme of Fluorite Deposits. International Journal of Geosciences 8, 599–610. https://doi.org/10.4236/ijg.2017.84032

Merlet, J.-C., Plassard, F., Chauvière, F.-X., 2016. L'art mobilier et la parure du gisement magdalénien d'Enval (Vic-le-Comte, Puy-de-Dôme). In: Cleyet-Merle, J.-J., Geneste, J.-M., Man-Estier, E. (Eds.), L'art au quotidien. Objets ornés du Paléolithique supérieur. Paleo: 401-423.

Naldrett, D.L., Lachaine, A., Naldrett, S.N., 1987. Rare-earth elements, thermal history, and the colour of natural fluorites. Canad. J. Earth Sci. 24, 2082-2088.

Odriozola, C.P.; Villalobos, R.; Burbidge, C.; Boaventura, R.; Sousa, A.C.; Rodríguez-Ariza, O.; Parilla-Giráldez, R., Prudêncio, M.I., Dias, M.I., 2016. Distribution and chronological framework for Iberian variscite mining and consumption at Pico Centeno, Encinasola, Spain. Quaternary Research 85, 159-176. http://dx.doi.org/10.1016/j.yqres.2015.11.010

Odriozola, C.P., Sousa, A.C., Mataloto, R., Boaventura, R., Andrade, M., Villalobos, R., Garrido-Cordero, J.A., Rodríguez, E., Martínez-Blanes, J.M., Avilés, M.A., Daura, J., Sanz, M. & Riquelme, J.A., 2019. Amber, beads and social interaction in the Late Prehistory of the Iberian Peninsula: an update. Archaeological and Anthropological Sciences, 11 (2): 567-595. https://doi.org/10.1007/s12520-017-0549-7

Polloni, A., 2008. Parures individuelles et sépultures collectives à la fin du Néolithique en Bassin parisien. Préhistoires Méditerranéennes14: 75-89. https://doi.org/10.4000/pm.324

Reimann, C., Filzmoser, P., Garrett, R.G., 2002. Factor analysis applied to regional geochemical data: Problems and possibilities. Appl. Geochem. 17 (3), 185-206. https://doi.org/10.1016/s0883-2927(01)00066-x

Roscian, S., Claustre, F., Dietrich, J.-E., 1992. Les parures du Midi méditerranéen du Néolithique ancien à l'Age du Bronze: origine et circulation des matières premières. Gallia préhistoire 34, 209-257.

Saintot, S., 2016. Contexte et pertinence des assemblages de Champ Madame. In: Saintot, S., Ballut, C., Bouby, L., Brisotto, V. et al. (Eds.), Un habitat chasséen en Auvergne: Champ Madame à Beaumont (Puy-de-Dôme) au Néolithique moyen II. Inrap. CNRS Éditions, Inrap, Chapitre 4 – Etude des mobiliers. Recherches archéologiques 11.

Smith, F.W., Hirst, D.M., 1974. Analysis of trace elements and fluid inclusions in fluorite from the Ardennes Massif. Ann. Soc. Géol. Belgique 97, 281-285.

Sun, S.S., McDonough, W.F., 1989. Chemical and isotopic systematic of oceanic basalts: implications for mantle composition and processes. In: Saunders, A.D., Norry, M.J. (Eds.), Magmatism in the ocean basins. Geol. Soc., Special Publication 42, 313-345.

Surmely, F., 2019. Objets de curiosité dans le site magdalénien d'Enval (Vic-le-Comte, Puy-de-Dôme, France). Paleo 30 (1), 244-254.

Swialkowski, M., 2020. Dans les calcaires du Givétien de l'Avesnois: la carrière "Le Cailloit", Glageon, Nord. Le Règne Minéral, Hors-série XXV/XXVI. Editions du Piat, 132-138.

Thomas, J., 1999. Understanding the Neolithic. London, Routledge.

Van Gijn, A., 2006. Ornaments of jet, amber and bone. In: Louwe Kooijmans, LP., Jongste, P.F.B. (Eds.), Schipluiden, A Neolithic settlement on the Dutch North Sea coast c. 3500 cal BC. Analecta Praehistorica Leidensia 37/38, 195-206.

Vanmontfort, B., Haesaerts, P., Jadin, I., 2003. Deux dates radiocarbone par AMS sur le gisement néolithique du Gué du Plantin (Neufvilles, Province du Hainaut, Belgique). Notae Praehistoricae 23, 173-179.

Vanmontfort, B., Geerts, A.-I., Casseyas, C., Bakels, C., Buydens, C., Damblon, F., Langohr, R., Van Neer, W., Vermeersch, P.M., 2001/2002. De Hel in de tweede helft van het 5de millenium v.Chr. Een midden-Neolithische enclosure te Spiere (prov. West-Vlaanderen). Archeologie in Vlaanderen 8, 9-77.

Vanmontfort, B., 2004. Converging Worlds. The Neolithisation of the Scheldt basin during the late fifth and early fourth millennium cal BC. PhD dissertation, KU Leuven.

Vanmontfort, B., 2006. Can we attribute the Middle Neolithic in the Scheldt and Middle Meuse Basins to the Michelsberg culture? In: Duhamel, P. (Ed.), Impacts interculturels au Néolithique moyen. Du terroir au territoire: sociétés et espaces, Actes du 25e colloque Interrégional sur le Néolithique (Dijon, 20-21 octobre 2001). Revue archéologique de l'Est, 25, 109-116.

Vanmontfort, B., 2001. The Group of Spiere as a new stylistic entity in the Middle Neolithic Scheldt Basin. Notae Praehistoricae 21, 139-143.

Vermeersch, P.M., Vynckier, G., Walter, R., 1990. Thieusies, ferme de l'Hosté, Site Michelsberg, II - Le matériel lithique. Studia Praehistorica Belgica 6, Leuven.

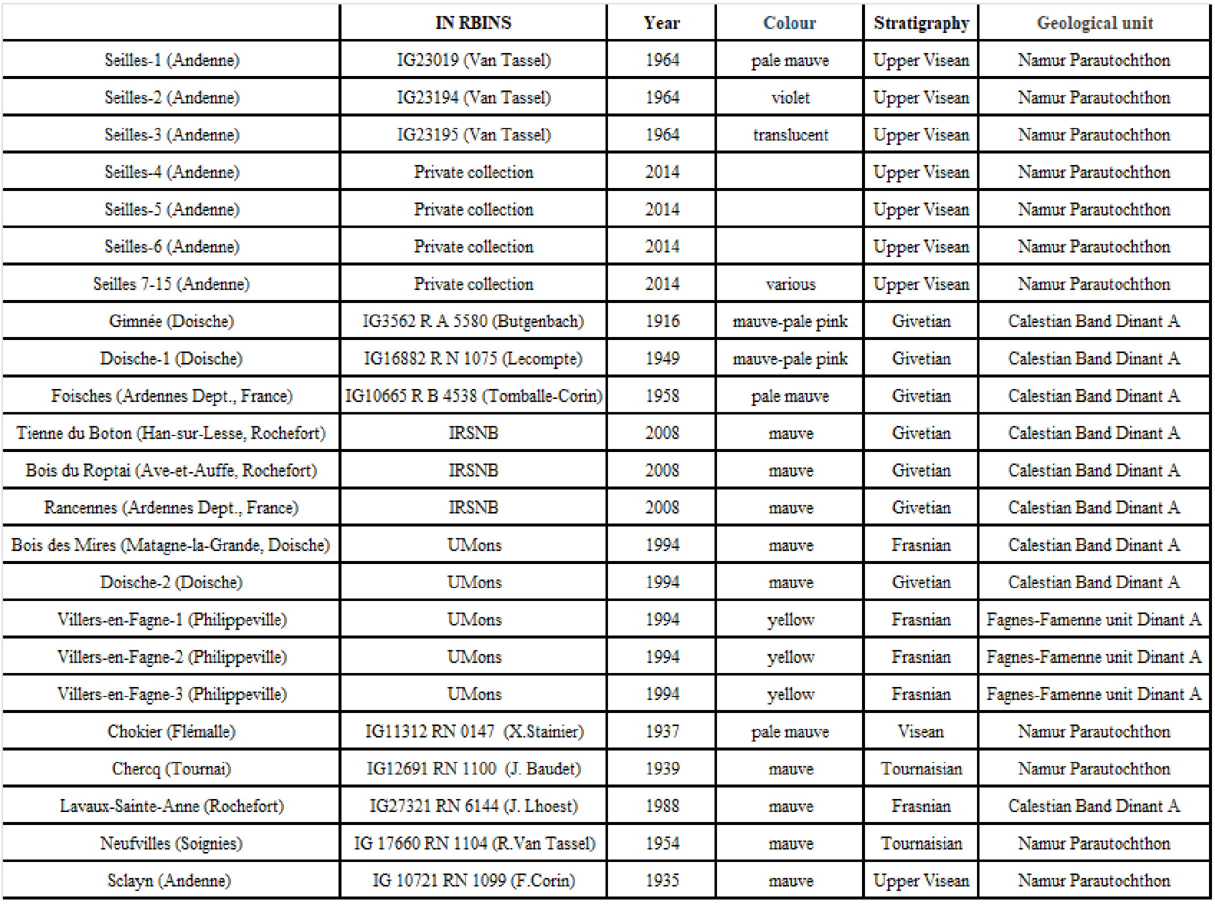

	IN RBINS	Year	Colour	Stratigraphy	Geological unit
Seilles-1 (Andenne)	IG23019 (Van Tassel)	1964	pale mauve	Upper Visean	Namur Parautochthon
Seilles-2 (Andenne)	IG23194 (Van Tassel)	1964	violet	Upper Visean	Namur Parautochthon
Seilles-3 (Andenne)	IG23195 (Van Tassel)	1964	translucent	Upper Visean	Namur Parautochthon
Seilles-4 (Andenne)	Private collection	2014		Upper Visean	Namur Parautochthon
Seilles-5 (Andenne)	Private collection	2014		Upper Visean	Namur Parautochthon
Seilles-6 (Andenne)	Private collection	2014		Upper Visean	Namur Parautochthon
Seilles 7-15 (Andenne)	Private collection	2014	various	Upper Visean	Namur Parautochthon
Gimnée (Doische)	IG3562 R A 5580 (Butgenbach)	1916	mauve-pale pink	Givetian	Calestian Band Dinant A
Doische-1 (Doische)	IG16882 R N 1075 (Lecompte)	1949	mauve-pale pink	Givetian	Calestian Band Dinant A
Foisches (Ardennes Dept., France)	IG10665 R B 4538 (Tomballe-Corin)	1958	pale mauve	Givetian	Calestian Band Dinant A
Tienne du Boton (Han-sur-Lesse, Rochefort)	IRSNB	2008	mauve	Givetian	Calestian Band Dinant A
Bois du Roptai (Ave-et-Auffe, Rochefort)	IRSNB	2008	mauve	Givetian	Calestian Band Dinant A
Rancennes (Ardennes Dept., France)	IRSNB	2008	mauve	Givetian	Calestian Band Dinant A
Bois des Mires (Matagne-la-Grande, Doische)	UMons	1994	mauve	Frasnian	Calestian Band Dinant A
Doische-2 (Doische)	UMons	1994	mauve	Givetian	Calestian Band Dinant A
Villers-en-Fagne-1 (Philippeville)	UMons	1994	yellow	Frasnian	Fagnes-Famenne unit Dinant A
Villers-en-Fagne-2 (Philippeville)	UMons	1994	yellow	Frasnian	Fagnes-Famenne unit Dinant A
Villers-en-Fagne-3 (Philippeville)	UMons	1994	yellow	Frasnian	Fagnes-Famenne unit Dinant A
Chokier (Flémalle)	IG11312 RN 0147 (X.Stainier)	1937	pale mauve	Visean	Namur Parautochthon
Chercq (Tournai)	IG12691 RN 1100 (J. Baudet)	1939	mauve	Tournaisian	Namur Parautochthon
Lavaux-Sainte-Anne (Rochefort)	IG27321 RN 6144 (J. Lhoest)	1988	mauve	Frasnian	Calestian Band Dinant A
Neufvilles (Soignies)	IG 17660 RN 1104 (R.Van Tassel)	1954	mauve	Tournaisian	Namur Parautochthon
Sclayn (Andenne)	IG 10721 RN 1099 (F.Corin)	1935	mauve	Upper Visean	Namur Parautochthon

Supporting Information 1

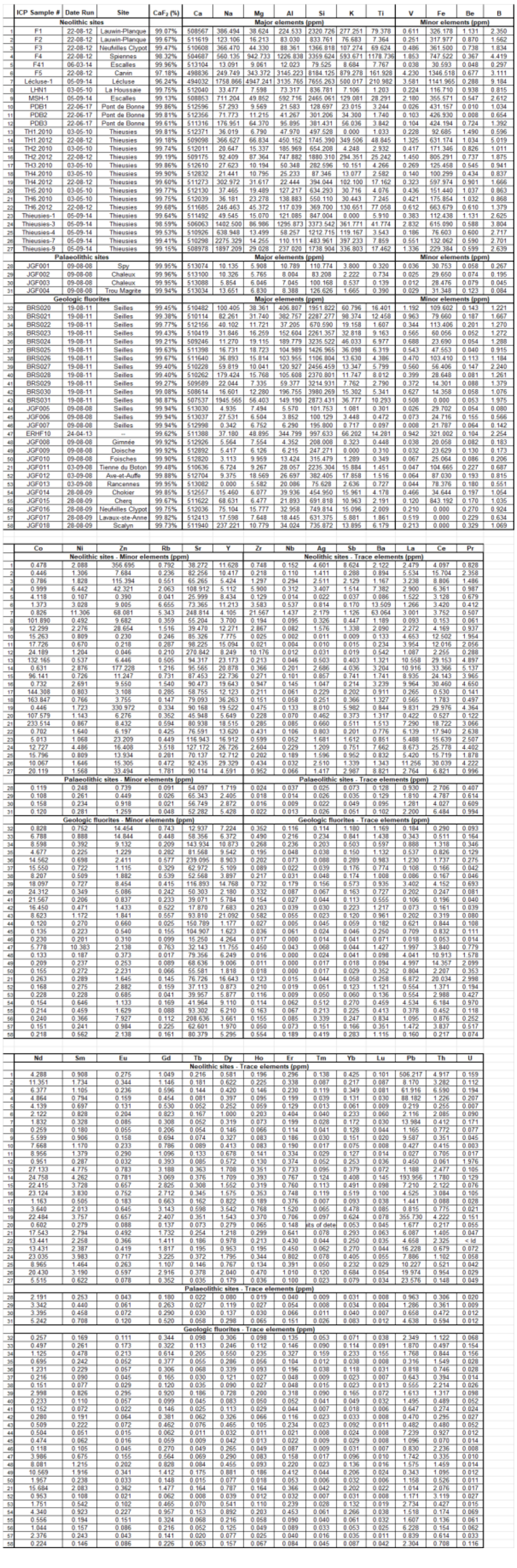

	ICP Sample #	Date Run	Site	CaF$_2$ (%)	Ca	Na	Mg	Al	Si	K	Ti	V	Fe	Be	B
	Neolithic sites				Major elements (ppm)							Minor elements (ppm)			
1	F1	22-08-12	Lauwin-Planque	99.07%	508567	386.494	38.624	224.533	2320.726	277.251	79.378	0.611	326.178	1.131	2.350
2	F2	22-08-12	Lauwin-Planque	99.67%	511619	123.106	16.213	83.030	833.761	76.683	7.364	0.251	317.977	0.870	1.562
3	F3	22-08-12	Neufvilles Clypot	99.47%	510608	366.470	44.330	88.361	1366.818	107.274	69.624	0.486	361.500	0.738	1.834
4	F4	22-08-12	Spiennes	98.32%	504687	560.135	942.733	1226.838	3359.624	593.671	1178.736	1.853	747.522	0.367	4.419
5	F41	06-03-14	Escalles	99.96%	513104	13.091	9.061	12.023	79.525	8.684	7.767	0.038	30.593	0.048	0.297
6	F5	22-08-12	Carvin	97.18%	498836	249.749	343.372	3145.223	8184.125	879.278	161.928	4.230	1346.518	0.677	3.111
7	Lécluse-1	05-09-14	Lécluse	96.24%	494032	1758.866	4947.241	3135.765	7655.263	500.017	210.982	3.581	1141.965	0.288	9.184
8	LHN1	03-05-10	La Houssaie	99.75%	512040	33.477	7.598	73.317	836.781	7.106	1.203	0.224	116.710	0.938	0.815
9	MSH-1	05-09-14	Escalles	99.13%	508853	711.204	49.852	592.716	2465.061	129.081	28.291	2.180	355.571	0.547	2.612
10	PDB1	22-06-17	Pont de Bonne	99.86%	512596	57.293	9.569	21.583	128.697	23.015	3.244	0.026	431.157	0.010	1.034
11	PDB2	22-06-17	Pont de Bonne	99.81%	512356	71.773	11.215	41.267	301.206	34.300	1.740	0.103	426.930	0.008	0.654
12	PDB3	22-06-17	Pont de Bonne	99.61%	511316	176.951	64.370	95.895	381.431	56.036	3.842	0.104	424.194	0.724	1.392
13	TH1.2010	03-05-10	Thieusies	99.81%	512371	36.019	6.790	47.970	497.528	0.000	1.033	0.228	92.685	1.490	0.596
14	TH1.2012	22-08-12	Thieusies	99.18%	509098	366.627	66.834	450.152	1745.390	349.506	48.845	1.325	631.174	1.034	5.019
15	TH2.2010	03-05-10	Thieusies	99.74%	512011	20.647	15.337	185.969	654.208	4.248	2.932	0.417	171.346	0.826	1.011
16	TH2.2012	22-08-12	Thieusies	99.19%	509175	92.409	87.364	747.882	1880.310	294.351	25.242	1.450	805.291	0.737	1.875
17	TH3.2010	03-05-10	Thieusies	99.86%	512610	27.623	10.194	50.348	282.596	10.151	4.266	0.269	125.458	0.545	0.941
18	TH4.2010	03-05-10	Thieusies	99.90%	512832	21.441	10.795	25.233	87.346	13.077	2.582	0.140	100.299	0.434	0.837
19	TH4.2012	22-08-12	Thieusies	99.60%	511273	302.972	31.617	22.444	394.044	102.100	17.162	0.323	597.974	0.901	1.666
20	TH5.2010	03-05-10	Thieusies	99.77%	512130	37.465	19.489	127.217	634.293	30.716	4.076	0.436	151.440	1.037	0.863
21	TH6.2010	03-05-10	Thieusies	99.75%	512039	36.181	23.278	138.883	550.110	30.443	7.245	0.421	175.854	1.032	0.868
22	TH6.2012	22-08-12	Thieusies	99.68%	511685	246.463	45.372	117.039	369.700	130.651	77.058	0.612	663.679	0.610	1.379
23	Thieusies-1	05-09-14	Thieusies	99.64%	511492	49.545	15.070	121.085	847.004	0.000	5.910	0.383	112.438	1.131	2.625
24	Thieusies-3	05-09-14	Thieusies	98.59%	506063	1402.500	86.986	1295.873	3373.542	361.771	41.774	2.832	615.090	0.588	3.804
25	Thieusies-4	05-09-14	Thieusies	99.53%	510926	638.948	13.499	58.257	1212.715	119.167	3.543	0.186	76.603	0.600	2.717
26	Thieusies-7	05-09-14	Thieusies	99.41%	510298	2275.329	14.255	110.111	483.961	397.233	7.859	0.551	132.062	0.590	2.701
27	Thieusies-9	05-09-14	Thieusies	99.15%	508978	1897.209	29.028	237.020	1738.904	336.803	17.462	1.336	229.384	0.599	2.639
	Palaeolithic sites				Major elements (ppm)							Minor elements (ppm)			
28	JGF001	09-08-08	Spy	99.95%	513074	10.135	5.908	10.789	110.774	3.800	0.320	0.036	30.753	0.058	0.267
29	JGF002	09-08-08	Chaleux	99.96%	513100	10.326	5.765	8.004	83.208	2.222	0.734	0.025	29.650	0.074	0.195
30	JGF003	09-08-08	Chaleux	99.95%	513088	5.854	6.046	7.045	100.168	0.537	0.139	0.012	28.476	0.079	0.045
31	JGF004	09-08-08	Trou Magrite	99.94%	513034	13.651	6.830	8.388	126.626	1.665	0.390	0.029	31.348	0.123	0.084
	Geologic fluorites				Major elements (ppm)							Minor elements (ppm)			
32	BRS020	19-08-11	Seilles	99.45%	510482	100.405	38.361	406.807	1951.822	60.796	16.401	1.192	109.602	0.143	1.221
33	BRS021	19-08-11	Seilles	99.38%	510114	82.261	31.740	382.757	2287.277	98.374	12.458	0.963	79.660	0.187	1.667
34	BRS022	19-08-11	Seilles	99.77%	512156	40.102	11.721	37.205	670.590	19.158	1.607	0.344	113.406	0.201	1.270
35	BRS023	19-08-11	Seilles	99.43%	510419	31.846	16.259	152.604	2261.357	32.818	9.163	0.565	60.056	0.052	1.272
36	BRS024	19-08-11	Seilles	99.21%	509246	11.270	19.115	189.779	3235.522	46.033	6.977	0.688	23.690	0.054	1.288
37	BRS025	19-08-11	Seilles	99.63%	511398	16.731	18.723	104.989	1426.965	36.098	6.319	0.543	47.553	0.040	0.915
38	BRS026	19-08-11	Seilles	99.67%	511640	36.893	15.814	103.955	1106.804	13.630	4.386	0.470	103.410	0.113	1.184
39	BRS027	19-08-11	Seilles	99.40%	510228	59.819	10.041	120.927	2456.459	13.347	5.799	0.560	56.406	0.147	2.240
40	BRS028	19-08-11	Seilles	99.40%	510262	179.424	15.768	105.608	2370.801	11.747	8.012	0.399	28.648	0.081	1.261
41	BRS029	19-08-11	Seilles	99.27%	509689	22.044	7.335	59.377	3214.931	7.762	2.790	0.372	14.301	0.088	1.379
42	BRS030	19-08-11	Seilles	99.08%	508614	16.601	12.280	196.755	3980.269	15.302	5.341	0.627	14.358	0.058	1.076
43	BRS031	19-08-11	Seilles	98.87%	507537	1945.565	56.403	149.190	2873.431	36.777	10.293	0.508	0.000	0.053	1.975
44	JGF005	09-08-08	Seilles	99.94%	513030	4.935	7.494	5.570	101.753	1.081	0.301	0.026	29.702	0.054	0.080
45	JGF006	09-08-08	Seilles	99.94%	513037	27.531	6.504	3.852	100.129	3.448	0.472	0.073	24.716	0.155	0.566
46	JGF007	09-08-08	Seilles	99.94%	512998	0.342	6.752	6.290	195.800	0.717	0.097	0.008	21.787	0.064	0.142
47	ERHF10	24-04-13	--	99.62%	511388	37.180	48.895	344.799	997.633	66.202	14.281	0.942	321.002	0.104	2.254
48	JGF008	09-08-08	Gimnée	99.92%	512926	5.564	7.554	4.352	208.008	0.323	0.448	0.038	20.058	0.082	0.183
49	JGF009	09-08-08	Doische	99.92%	512892	5.417	6.126	6.215	247.271	0.000	0.310	0.032	23.629	0.130	0.173
50	JGF010	09-08-08	Foisches	99.90%	512820	3.113	9.959	13.424	315.479	1.289	0.349	0.067	25.064	0.086	0.206
21	JGF011	03-09-08	Tienne du Boton	99.48%	510636	6.724	9.267	28.057	2235.304	15.884	1.451	0.047	104.665	0.227	0.687
52	JGF012	03-09-08	Ave-et-Auffe	99.88%	512704	9.375	18.569	26.697	382.405	17.858	1.516	0.064	87.030	0.193	0.815
53	JGF013	03-09-08	Rancennes	99.95%	513082	0.000	5.582	20.086	75.628	2.636	0.727	0.044	78.376	0.180	0.551
54	JGF014	28-08-09	Chokier	99.85%	512557	15.460	6.077	39.936	454.950	15.961	4.178	0.466	34.644	0.197	1.054
55	JGF015	28-08-09	Cherq	99.67%	511622	68.631	6.477	21.893	691.818	10.963	2.191	0.120	843.192	0.170	1.035
56	JGF016	28-08-09	Neufvilles Clypot	99.75%	512036	75.104	15.777	32.958	749.814	15.096	2.009	0.210	0.000	0.270	0.924
57	JGF017	28-08-09	Lavaux-ste-Anne	99.82%	512413	17.598	7.648	18.445	631.375	5.881	1.861	0.519	0.000	0.229	0.634
58	JGF018	28-08-09	Scalyn	99.73%	511940	237.221	10.779	34.024	735.872	13.895	6.179	0.213	0.000	0.329	1.069

	Co	Ni	Zn	Rb	Sr	Y	Zr	Nb	Ag	Sb	Ba	La	Ce	Pr
	Neolithic sites - Minor elements (ppm)						Neolithic sites - Trace elements (ppm)							
1	0.478	2.088	356.695	0.792	38.272	11.628	0.748	0.152	4.601	8.624	2.122	2.479	4.097	0.828
2	0.446	1.306	7.684	0.236	82.256	10.417	0.218	0.110	1.411	0.288	0.894	5.534	15.704	2.358
3	0.786	1.828	115.394	0.551	65.265	5.424	1.297	0.294	2.511	2.129	1.167	3.238	8.806	1.486
4	0.999	6.442	42.321	2.063	108.912	5.112	5.900	0.312	3.407	1.514	7.382	2.900	6.361	0.987
5	4.118	0.107	0.390	0.041	25.999	8.434	0.129	0.014	0.022	0.037	0.086	1.522	3.128	0.679
6	1.373	3.028	9.005	6.655	73.365	11.213	3.583	0.537	0.814	0.170	13.509	1.266	3.420	0.412
7	0.826	11.306	68.081	5.343	248.814	4.105	21.567	1.437	2.179	1.126	63.064	3.001	3.752	0.507
8	101.890	0.492	9.682	0.359	55.204	3.700	0.194	0.095	0.326	0.447	1.189	0.093	0.153	0.061
9	12.299	2.276	28.654	1.516	39.470	12.271	2.867	0.082	1.576	1.338	2.090	2.272	4.169	0.937
10	15.263	0.809	0.230	0.246	85.326	7.775	0.025	0.002	0.011	0.009	0.133	4.653	12.502	1.954
11	17.726	0.670	0.218	0.287	98.225	15.094	0.021	0.004	0.010	0.015	0.234	3.954	12.016	2.056
12	24.189	1.204	0.046	0.210	270.842	8.249	10.176	0.012	0.031	0.019	0.542	1.087	2.255	0.288
13	132.165	0.537	6.446	0.505	94.317	23.173	0.213	0.046	0.503	0.403	1.321	10.558	29.153	4.897
14	0.631	2.876	177.228	1.216	95.565	20.878	0.366	0.201	2.686	4.036	3.204	10.916	33.366	5.137
15	96.141	0.726	11.247	0.731	87.453	22.736	0.271	0.101	0.857	0.741	1.741	8.935	24.143	3.965
16	0.732	2.691	9.550	1.540	90.473	19.643	0.947	0.145	1.047	0.214	3.239	9.964	30.460	4.650
17	144.308	0.803	3.108	0.285	58.755	12.123	0.211	0.061	0.229	0.202	0.911	0.265	0.530	0.141
18	163.847	0.766	3.755	0.147	79.093	36.263	0.151	0.058	0.251	0.366	1.327	0.565	1.783	0.497
19	0.446	1.723	330.972	0.334	90.168	19.522	0.475	0.133	8.010	5.982	0.844	9.831	29.976	4.364
20	107.579	1.143	6.276	0.352	45.948	5.649	0.228	0.070	0.462	0.373	1.317	0.422	0.527	0.122
21	233.514	0.867	8.432	0.594	80.938	18.515	0.285	0.085	0.660	0.511	1.513	7.290	18.722	3.066
22	0.702	1.640	6.197	0.425	76.591	13.620	0.431	0.106	0.803	0.201	0.776	6.139	17.940	2.638
23	5.013	1.068	23.209	0.449	116.943	16.912	0.599	0.052	1.681	1.612	0.851	5.488	15.639	2.507
24	12.727	4.486	16.408	3.518	127.172	26.726	2.604	0.229	1.209	0.751	7.662	8.673	25.778	4.402
25	15.796	0.809	13.934	0.281	70.137	12.712	0.202	0.189	1.596	0.952	0.832	5.420	15.719	1.878
26	10.067	1.646	15.305	0.472	92.435	29.329	0.434	0.032	2.510	1.339	1.343	11.256	30.039	4.222
27	20.119	1.568	33.494	1.781	90.114	4.591	0.952	0.066	1.417	2.987	8.821	2.764	6.821	0.996
	Palaeolithic sites - Minor elements (ppm)						Palaeolithic sites - Trace elements (ppm)							
28	0.119	0.248	0.739	0.091	54.097	1.719	0.024	0.037	0.025	0.073	0.128	0.930	2.706	0.407
29	0.108	0.261	0.449	0.026	65.343	2.405	0.018	0.014	0.026	0.035	0.129	1.810	4.787	0.614
30	0.158	0.234	0.918	0.021	56.749	2.872	0.016	0.009	0.022	0.049	0.095	1.281	4.027	0.609
31	0.120	0.281	1.259	0.048	52.282	5.428	0.022	0.013	0.026	0.051	0.102	2.200	6.484	0.994
	Geologic fluorites - Minor elements (ppm)						Geologic fluorites - Trace elements (ppm)							
32	0.828	0.752	14.454	0.743	12.937	7.224	0.352	0.116	0.114	1.180	1.169	0.184	0.290	0.093
33	6.788	0.888	14.844	0.448	58.356	6.372	0.490	0.216	0.234	0.841	1.438	0.343	0.511	0.164
34	8.598	0.392	9.132	0.209	143.934	10.873	0.268	0.236	0.203	0.503	0.597	0.888	1.318	0.346
35	4.677	0.225	1.229	0.282	81.568	9.542	0.195	0.048	0.038	0.150	1.132	0.537	0.826	0.129
36	14.562	0.698	2.411	0.577	239.095	8.903	0.202	0.073	0.088	0.289	0.983	1.230	1.737	0.275
37	15.550	0.722	1.115	0.329	62.972	5.109	0.089	0.022	0.039	0.176	0.774	0.108	0.166	0.042
38	8.207	0.509	1.882	0.539	52.568	3.897	0.217	0.031	0.048	0.174	1.008	0.086	0.167	0.046
39	18.097	0.727	8.454	0.415	116.893	14.768	0.732	0.179	0.156	0.573	0.935	3.402	4.152	0.693
40	24.312	0.349	5.086	0.242	50.303	2.180	0.332	0.087	0.067	0.163	0.727	0.202	0.247	0.081
41	21.567	0.206	0.837	0.233	39.071	5.784	0.154	0.027	0.044	0.113	0.555	0.106	0.196	0.040
42	16.450	0.471	1.433	0.522	17.870	7.683	0.203	0.039	0.030	0.223	1.217	0.073	0.161	0.039
43	8.623	1.172	1.841	0.557	93.810	21.092	0.582	0.055	0.023	0.120	0.961	0.202	0.319	0.080
44	0.120	0.270	0.660	0.025	150.789	1.177	0.027	0.005	0.045	0.059	0.182	0.621	0.844	0.108
45	0.135	0.223	0.540	0.155	104.907	1.623	0.036	0.061	0.024	0.046	0.250	0.709	0.832	0.111
46	0.230	0.201	0.310	0.099	15.250	4.264	0.017	0.000	0.014	0.041	0.071	0.018	0.053	0.014
47	5.778	10.383	2.138	0.763	32.143	11.755	0.450	0.043	0.068	0.044	1.427	1.997	3.840	0.779
48	0.133	0.187	0.373	0.017	79.356	6.249	0.016	0.000	0.024	0.041	0.098	4.041	10.913	1.578
49	0.209	0.237	0.253	0.089	68.636	9.006	0.011	0.000	0.017	0.018	0.094	4.997	14.357	2.099
50	0.155	0.272	2.231	0.066	55.581	1.818	0.018	0.000	0.017	0.029	0.352	0.804	2.207	0.353
21	0.263	0.289	1.645	0.145	76.726	16.643	0.123	0.015	0.044	0.058	0.258	6.872	20.034	2.998
52	0.168	0.275	2.882	0.159	37.113	0.873	0.210	0.019	0.051	0.123	1.121	0.554	1.371	0.194
53	0.228	0.228	0.685	0.041	39.957	5.877	0.116	0.009	0.050	0.060	0.136	0.554	2.988	0.427
54	0.154	0.646	1.133	0.169	41.964	9.110	0.114	0.062	0.512	0.270	0.459	4.534	6.184	0.970
55	0.214	0.459	1.629	0.088	93.302	6.210	0.163	0.067	0.213	0.225	0.413	0.378	0.452	0.118
56	0.240	0.366	7.927	0.112	208.636	3.661	0.155	0.085	0.339	0.247	0.834	1.095	0.876	0.252
57	0.151	0.241	0.984	0.225	62.601	1.970	0.050	0.073	0.151	0.166	0.351	1.472	3.837	0.517
58	0.218	0.562	2.138	0.161	80.379	5.295	0.554	0.189	0.419	0.283	1.115	0.160	0.217	0.074

	Nd	Sm	Eu	Gd	Tb	Dy	Ho	Er	Tm	Yb	Lu	Pb	Th	U
	Neolithic sites - Trace elements (ppm)													
1	4.288	0.908	0.275	1.049	0.216	0.581	0.196	0.296	0.138	0.425	0.101	506.217	4.917	0.159
2	11.351	1.734	0.344	1.146	0.181	0.622	0.225	0.338	0.087	0.217	0.087	8.170	3.282	0.112
3	6.377	1.105	0.236	0.596	0.144	0.420	0.146	0.230	0.119	0.349	0.081	61.916	6.590	0.194
4	4.864	0.794	0.159	0.454	0.081	0.397	0.095	0.199	0.039	0.131	0.030	88.182	1.226	0.207
5	4.139	0.697	0.131	0.530	0.052	0.252	0.059	0.129	0.013	0.061	0.009	0.219	0.255	0.007
6	2.122	0.828	0.204	0.823	0.167	1.000	0.203	0.404	0.040	0.233	0.060	2.116	2.085	0.090
7	1.832	0.328	0.085	0.308	0.052	0.319	0.073	0.199	0.028	0.172	0.030	13.984	0.412	0.171
8	0.259	0.180	0.055	0.206	0.054	0.146	0.066	0.114	0.041	0.128	0.044	1.165	0.772	0.077
9	5.599	0.906	0.158	0.694	0.074	0.327	0.083	0.186	0.030	0.151	0.020	9.587	0.351	0.045
10	7.668	1.170	0.233	0.786	0.089	0.413	0.083	0.190	0.017	0.075	0.008	0.427	0.415	0.003
11	8.956	1.379	0.290	1.096	0.133	0.678	0.141	0.334	0.029	0.127	0.014	0.027	0.705	0.017
12	0.951	0.287	0.032	0.393	0.085	0.572	0.130	0.374	0.052	0.253	0.036	0.450	0.061	1.976
13	27.133	4.775	0.783	3.188	0.363	1.708	0.351	0.733	0.095	0.379	0.072	1.188	2.477	0.105
14	24.758	4.262	0.781	3.069	0.376	1.709	0.393	0.767	0.124	0.408	0.145	193.956	1.780	0.129
15	22.415	3.728	0.657	2.825	0.308	1.552	0.319	0.760	0.113	0.491	0.098	7.210	2.122	0.076
16	23.124	3.830	0.752	2.712	0.345	1.575	0.353	0.748	0.119	0.519	0.100	4.525	3.084	0.105
17	1.163	0.505	0.183	0.663	0.162	0.822	0.189	0.376	0.007	0.093	0.038	1.441	0.088	0.028
18	3.640	2.013	0.645	3.143	0.598	3.542	0.768	1.520	0.065	0.478	0.085	0.815	0.775	0.021
19	22.484	3.757	0.657	2.407	0.351	1.543	0.370	0.706	0.097	0.624	0.078	355.730	4.222	0.151
20	0.602	0.279	0.088	0.137	0.073	0.279	0.065	0.148	its of dete	0.053	0.045	1.677	0.217	0.055
21	17.543	2.794	0.492	1.732	0.254	1.218	0.299	0.641	0.078	0.293	0.063	6.087	1.405	0.047
22	13.441	2.258	0.366	1.411	0.186	0.978	0.213	0.430	0.044	0.250	0.035	4.658	2.325	< ld
23	13.431	2.387	0.419	1.817	0.195	0.953	0.195	0.450	0.062	0.270	0.044	16.228	0.679	0.072
24	23.035	3.983	0.717	3.225	0.372	1.795	0.344	0.802	0.078	0.405	0.055	7.886	1.102	0.058
25	8.965	1.464	0.263	1.107	0.146	0.767	0.134	0.391	0.050	0.232	0.029	10.227	0.521	0.042
26	20.430	3.190	0.597	2.916	0.378	2.040	0.470	1.010	0.120	0.684	0.054	19.974	0.954	0.029
27	5.515	0.622	0.078	0.352	0.035	0.179	0.036	0.100	0.023	0.079	0.034	23.576	0.148	0.049
	Palaeolithic sites - Trace elements (ppm)													
28	2.191	0.253	0.043	0.180	0.022	0.080	0.019	0.040	0.009	0.031	0.008	0.963	0.306	0.020
29	3.342	0.440	0.061	0.263	0.027	0.119	0.027	0.054	0.008	0.034	0.004	1.286	0.361	0.009
30	3.395	0.458	0.072	0.290	0.030	0.137	0.030	0.066	0.011	0.040	0.007	0.658	0.472	0.012
31	5.242	0.708	0.120	0.520	0.058	0.298	0.065	0.151	0.026	0.083	0.012	4.638	0.594	0.012
	Geologic fluorites - Trace elements (ppm)													
32	0.257	0.169	0.111	0.344	0.098	0.306	0.098	0.135	0.053	0.071	0.038	2.349	1.122	0.068
33	0.497	0.261	0.173	0.322	0.113	0.246	0.112	0.146	0.090	0.114	0.091	1.870	0.497	0.154
34	1.125	0.478	0.213	0.614	0.205	0.550	0.235	0.327	0.159	0.233	0.155	1.768	0.844	0.156
35	0.695	0.242	0.052	0.377	0.055	0.286	0.056	0.104	0.012	0.038	0.008	0.316	1.549	0.028
36	1.231	0.229	0.057	0.306	0.068	0.339	0.093	0.196	0.038	0.118	0.031	0.818	0.746	0.028
37	0.216	0.090	0.045	0.165	0.030	0.121	0.027	0.048	0.009	0.023	0.007	0.643	0.394	0.014
38	0.151	0.077	0.029	0.120	0.035	0.090	0.027	0.048	0.015	0.023	0.013	0.555	2.214	0.026
39	2.998	0.826	0.295	0.920	0.186	0.728	0.200	0.318	0.090	0.165	0.072	1.613	1.317	0.098
40	0.233	0.110	0.057	0.099	0.045	0.083	0.050	0.052	0.041	0.049	0.032	1.495	0.489	0.052
41	0.152	0.072	0.022	0.146	0.025	0.113	0.029	0.044	0.007	0.018	0.006	0.647	0.274	0.024
42	0.280	0.191	0.064	0.381	0.062	0.326	0.066	0.116	0.023	0.033	0.008	0.470	0.295	0.027
43	0.509	0.222	0.072	0.462	0.076	0.465	0.105	0.234	0.023	0.092	0.011	0.482	0.480	0.052
44	0.504	0.051	0.015	0.062	0.011	0.032	0.011	0.021	0.008	0.024	0.008	7.239	0.927	0.012
45	0.474	0.062	0.016	0.059	0.009	0.042	0.013	0.022	0.009	0.029	0.008	1.096	0.070	0.014
46	0.118	0.105	0.045	0.270	0.049	0.265	0.049	0.087	0.009	0.031	0.007	0.830	2.236	0.008
47	3.986	0.675	0.155	0.564	0.069	0.290	0.083	0.158	0.017	0.096	0.010	1.742	0.335	0.010
48	8.081	1.215	0.202	0.828	0.084	0.455	0.093	0.220	0.023	0.136	0.016	1.575	1.459	0.014
49	10.569	1.916	0.341	1.412	0.175	0.881	0.186	0.412	0.044	0.206	0.024	0.343	1.095	0.012
50	1.957	0.238	0.033	0.148	0.015	0.077	0.018	0.053	0.006	0.032	0.006	1.158	0.526	0.011
21	15.684	2.083	0.362	1.477	0.164	0.787	0.164	0.366	0.042	0.202	0.022	1.014	2.076	0.017
52	0.953	0.108	0.021	0.062	0.008	0.039	0.012	0.032	0.007	0.031	0.008	1.171	3.119	0.027
53	1.751	0.542	0.102	0.465	0.070	0.541	0.110	0.239	0.028	0.132	0.019	2.734	0.427	0.015
54	4.340	0.923	0.227	0.957	0.153	0.892	0.203	0.453	0.061	0.266	0.038	1.518	0.174	0.069
55	0.556	0.194	0.151	0.324	0.068	0.216	0.058	0.090	0.040	0.061	0.032	1.607	0.136	0.061
56	1.044	0.157	0.086	0.216	0.052	0.125	0.049	0.089	0.033	0.053	0.025	6.228	0.154	0.062
57	2.376	0.243	0.043	0.141	0.020	0.077	0.025	0.040	0.016	0.035	0.011	0.839	0.614	0.033
58	0.224	0.146	0.086	0.226	0.063	0.157	0.067	0.084	0.045	0.087	0.042	2.304	0.708	0.116

Supporting Information 2

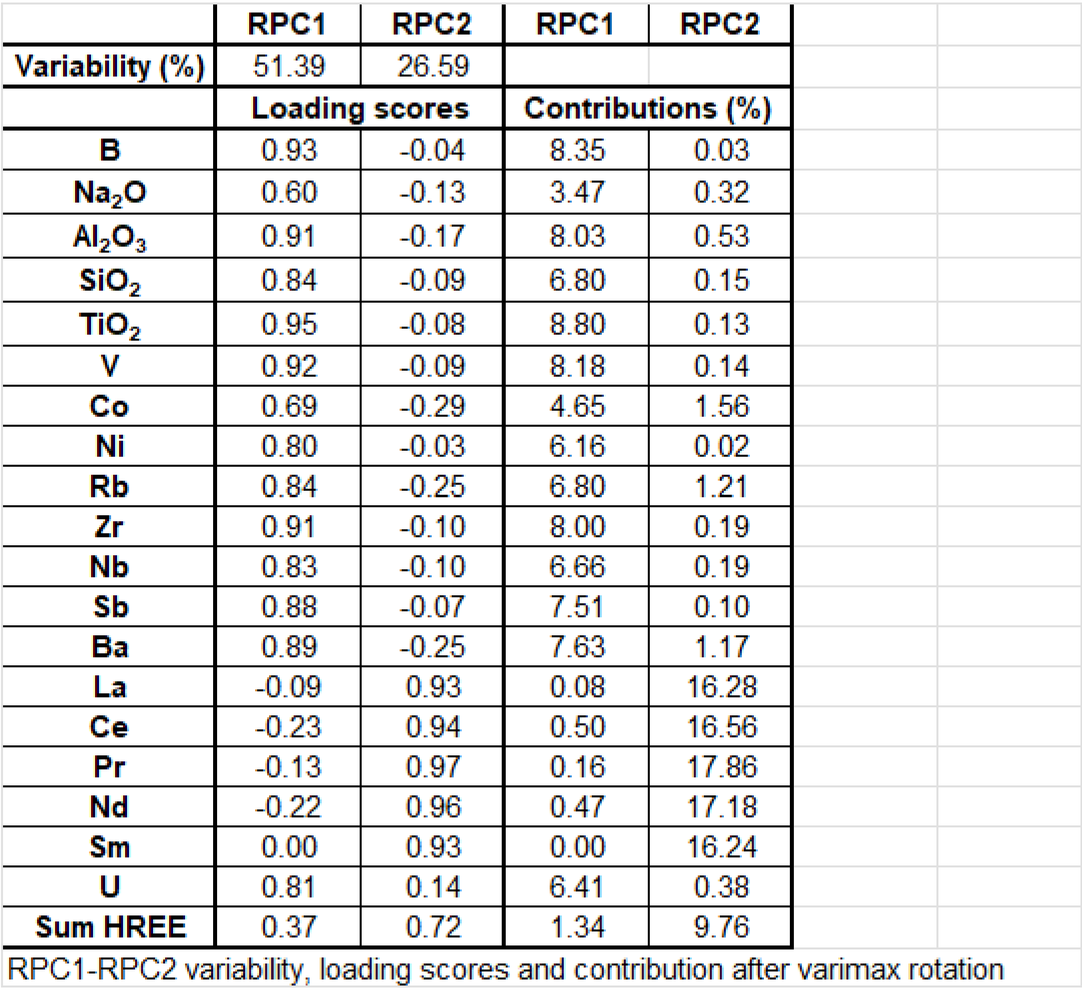

	RPC1	RPC2	RPC1	RPC2
Variability (%)	51.39	26.59		
	Loading scores		Contributions (%)	
B	0.93	-0.04	8.35	0.03
Na_2O	0.60	-0.13	3.47	0.32
Al_2O_3	0.91	-0.17	8.03	0.53
SiO_2	0.84	-0.09	6.80	0.15
TiO_2	0.95	-0.08	8.80	0.13
V	0.92	-0.09	8.18	0.14
Co	0.69	-0.29	4.65	1.56
Ni	0.80	-0.03	6.16	0.02
Rb	0.84	-0.25	6.80	1.21
Zr	0.91	-0.10	8.00	0.19
Nb	0.83	-0.10	6.66	0.19
Sb	0.88	-0.07	7.51	0.10
Ba	0.89	-0.25	7.63	1.17
La	-0.09	0.93	0.08	16.28
Ce	-0.23	0.94	0.50	16.56
Pr	-0.13	0.97	0.16	17.86
Nd	-0.22	0.96	0.47	17.18
Sm	0.00	0.93	0.00	16.24
U	0.81	0.14	6.41	0.38
Sum HREE	0.37	0.72	1.34	9.76

RPC1-RPC2 variability, loading scores and contribution after varimax rotation

Supporting information 3